

FLUORESCENCE SPECTROSCOPY OF
FOSCAN[®] INDUCED FELINE
TISSUES

By

SAMUEL JAMES RHOADES IV

Bachelor of Science

Loyola University

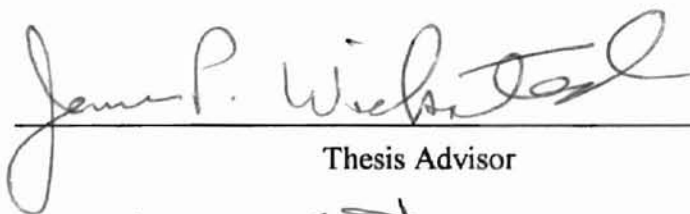
New Orleans, Louisiana

1997

Submitted to the Faculty of the
Graduate College of the
Oklahoma State University
in partial fulfillment of
the requirements for
the Degree of
MASTER OF SCIENCE
December, 1999

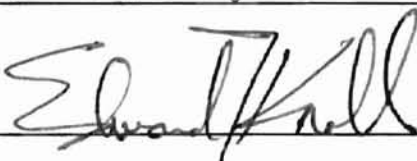
FLUORESCENCE SPECTROSCOPY OF
FOSCAN[®] INDUCED FELINE
TISSUES

Thesis Approved:



Thesis Advisor





Wayne B. Powell

Dean of the Graduate College

ACKNOWLEDGEMENTS

I would like to express my heartfelt appreciation to my major advisor, Dr. James P. Wicksted for his patience, generosity and guidance. I also would like to recognize Dr. Kenneth E. Bartels for allowing me the opportunity to study medical applications of lasers in the Boren Veterinary Medical Teaching Hospital, and for providing the bulk of my experimental ideas. I sincerely appreciate Dr. Edward T. Knobbe for serving on my graduate committee. I would like to show my gratitude to Dr. Bartels, Dr. Wicksted, and the Department of Physics for the generous financial support that I received while enrolled at Oklahoma State.

Moreover, I wish to express my sincere gratitude to those who provided suggestions and assistance for this study: Dr. Christopher S. Arnold, Dr. Abdulatif Y. Hamad, Dr. Gregory A. Campbell, and Dr. Avigdor M. Ronn.

This research project was done in conjunction with a Phase I study in the Sarkey's Biomedical Laser Lab at the Boren Veterinary Medical Teaching Hospital at Oklahoma State University to study the biodistribution of Foscan[®] in the cat.

I would also like to thank my family and friends for giving me the strength to persevere when all seemed lost. I truly believe that without your help I would not have been able to achieve any of my dreams.

TABLE OF CONTENTS

Chapter	Page
1. INTRODUCTION	1
1.1 History of Photodynamic Therapy	1
1.2 History of meta-Tetra(hydroxyphenyl) chlorin	2
1.3 Optical Properties of meta-Tetra(hydroxyphenyl) chlorin	3
1.4 Back Scattered Fluorescence	4
1.5 Contributions of This Thesis	5
2. EXPERIMENTAL PROCEDURES	10
2.1 Introduction	10
2.2 Sample Preparation (Animal)	10
2.3 Experimental Setup and Sample Preparation	12
3. RESULTS AND DISCUSSION.....	19
3.1 Introduction	19
3.2 Kidney Data Analysis.....	20
3.3 Liver Data Analysis.....	21
3.4 Lung Data Analysis	22
3.5 Nasal Planum Data Analysis	23
3.6 Thyroid Data Analysis.....	24
3.7 Discussion.....	25
3.7.1 Introduction.....	25
3.7.2 Long Island Jewish Medical Center	26
4. SUMMARY.....	59
REFERENCES.....	61

LIST OF TABLES

Table	Page
2.1 Cats and tissue harvesting time for animals injected with 0.15 mg/kg	15
2.2 Cats and tissue harvesting time for animals injected with 0.30 mg/kg	16
2.3 Cats and tissue harvesting time for animals injected with 0.60 mg/kg	17
3.1 PeakFit statistical analysis data for feline kidney.....	28
3.2 PeakFit statistical analysis data for feline liver.....	29
3.3 PeakFit statistical analysis data for feline lung.....	30
3.4 PeakFit statistical analysis data for feline nasal planum.....	31
3.5 PeakFit statistical analysis data for feline thyroid.....	32
3.6 Results of biodistribution study of Foscan [®] performed by Dr. Ronn's group at Long Island Jewish Medical Center.....	33

Figure	page
3.1 Emission spectra of kidney not injected with Foscan [®]	46
3.1 Emission spectra of kidney injected with 0.15 mg/kg of Foscan [®]	47
LIST OF FIGURES	
3.1 Emission spectra of kidney injected with 0.30 mg/kg of Foscan [®]	48

Figure	Page
1.1 Chemical structure for meta-tetra(hydroxyphenyl) chlorin.	6
1.2 Illustration of processes relevant to the energy concepts of fluorescence.....	7
1.3 Fluorescence-excitation spectra of meta-tetra(hydroxyphenyl) chlorin, Photofrin II [®] and meso-tetra-hydroxyphenyl-porphyrin.....	8
1.4 The molecular basis for HpD fluorescence and photodynamic action.....	9
2.1 Experimental setup.	18
3.1 Example of method used to determine calculation of autofluorescence (kidney).	34
3.2a Fitting demonstration for peak, FWHM and center analyzation of liver data (24 hours, 0.60 mg/kg).	35
3.2b Fitting demonstration for peak, FWHM and center analyzation of liver data (24 hours, 0.60 mg/kg).	36
3.3 Emission spectra of kidney not injected with Foscan [®]	37
3.4 Emission spectra of kidney injected with 0.15 mg/kg of Foscan [®]	38
3.5 Emission spectra of kidney injected with 0.30 mg/kg of Foscan [®]	39
3.6 Emission spectra of kidney injected with 0.60 mg/kg of Foscan [®]	40
3.7 Emission spectra of liver not injected with Foscan [®]	41
3.8 Emission spectra of liver injected with 0.15 mg/kg of Foscan [®]	42
3.9 Emission spectra of liver injected with 0.30 mg/kg of Foscan [®]	43
3.10a Emission spectra of liver injected with 0.60 mg/kg of Foscan [®]	44
3.10b Normalized emission spectra of liver injected with 0.60 mg/kg of Foscan [®]	45

Figure	page
3.11 Emission spectra of lung not injected with Foscan®	46
3.12 Emission spectra of lung injected with 0.15 mg/kg of Foscan®	47
3.13 Emission spectra of lung injected with 0.30 mg/kg of Foscan®	48
3.14 Emission spectra of lung injected with 0.60 mg/kg of Foscan®	49
3.15 Emission spectra of nasal planum not injected with Foscan®	50
3.16 Emission spectra of nasal planum injected with 0.15 mg/kg of Foscan®	51
3.17 Emission spectra of nasal planum injected with 0.30 mg/kg of Foscan®	52
3.18 Emission spectra of nasal planum injected with 0.60 mg/kg of Foscan®	53
3.19 Emission spectra of thyroid not injected with Foscan®	54
3.20 Emission spectra of thyroid injected with 0.15 mg/kg of Foscan®	55
3.21 Emission spectra of thyroid injected with 0.30 mg/kg of Foscan®	56
3.22 Emission spectra of thyroid injected with 0.60 mg/kg of Foscan®	57
3.23 Plot of maximum fluorescent intensity versus necropsy time for kidney tissues.. ..	58

NOMENCLATURE

SYMBOLS

PHOTODYNAMIC THERAPY

HpD	haematoporphyrin derivative
FWHM	full width half maximum
mTHPC	meta-tetra(hydroxyphenyl) chlorin
PDT	Photodynamic Therapy
PMT	Photomultiplier tube

CHAPTER 1

INTRODUCTION

1.1 HISTORY OF PHOTODYNAMIC THERAPY

Photodynamic therapy (PDT) is an emerging modality for the treatment of cancerous tumors. PDT is a non-thermal, photochemical technique that involves the local activation of a preadministered photosensitizer by light. The wavelength of this light is matched to an absorption peak of the photosensitizer being used (Mlkvy *et al.*, 1997). The idea to utilize photosensitization to treat cancer has been around since 1966, when Dr. Richard Lipson treated one patient with hematoporphyrin derivative (HpD) for tumor response of a metastatic cancer in the breast (Lipson *et al.*, 1966). Usually a non-invasive technique, PDT has the advantage of being minimally destructive to all non-diseased tissue in the surrounding area, due to selective retention of the drug in the tumor tissue. To attain optimal success, the destruction of the non-diseased tissue must be minimized while the destruction of the diseased tissue should be maximized. PDT treatments involve the concerted action of a photosensitive chemical compound and an activating light (usually a monochromatic, collimated, coherent beam of laser light), neither of which can alone affect the intended target tissue. However, when these components are combined properly, photochemically induced tumor destruction takes place at the mitochondrial level, mainly through the production of singlet oxygen (Weishaupt *et al.*, 1976).

1.2 HISTORY OF META-TETRA(HYDROXYPHENYL) CHLORIN

Meta-tetra(hydroxyphenyl) chlorin (mTHPC), also known as Temoporfin, or by its trade name of Foscan[®], is a second-generation photosensitizer. It is a “hard drug” that is not metabolized, but is nearly completely eliminated via the liver. The Foscan[®] used in our studies was obtained from Scotia Pharmaceuticals (Guildford, Surrey, UK). The drug, supplied as a sterile lyophilized powder, was dissolved in a diluent, which was a mixture of 50% ethanol and 50% sterile water, to a final concentration of 2.5 mg/ml.

The advantages that mTHPC has over other photosensitizers, such as HpD, Photofrin II[®] (Lederle Parenterals, Carolina, Puerto Rico) and meso-tetra-hydroxyphenylporphyrin, include its high selectivity, high fluorescence quantum yield, relatively high absorption in the red region of visible light at 652 nm and minimal photosensitivity (Ma *et al.*, 1994). Many of the other photosensitizers have the considerable disadvantage of causing skin photosensitivity that can last up to two or three months (Dougherty *et al.*, 1990), whereas mTHPC's lasts only a two to three weeks (Dougherty, 1993). Foscan[®] is preferentially accumulated in tumor tissue (up to twenty times higher than in normal tissue), and moreover, a photodynamic therapeutic ratio of 200:1 (damage of tumor tissue to damage of normal tissue) has been shown in animal models (Stewart, 1993). It has also been noticed that mTHPC shows an interpatient variation of drug accumulation in normal and malignant tissue (Braichotte *et al.*, 1996a, Braichotte *et al.*, 1996b).

1.3 OPTICAL PROPERTIES OF META-TETRA(HYDROXYPHENYL) CHLORIN

The photobiology of a drug is related to its chemical structure (Berenbaum, 1989). The optical properties of meta-tetra(hydroxyphenyl) chlorin differ slightly from similar second-generation photosensitizers such as Photofrin II[®] and meso-tetra-hydroxyphenyl-porphyrin. The difference is a variance in chemical structure of the compounds. The peculiarity is that for mTHPC, one of the double bonds is reduced to a single bond (Ma *et al.*, 1994). Figure 1.1 shows the chemical structure of the mTHPC molecule.

It has been reported that the penetration depth of light into soft tissues is maximal at larger wavelengths (Hammer-Wilson *et al.*, 1998, Hammer-Wilson *et al.*, 1999). Foscan[®] has a large absorption peak at 652 nm and a smaller one at 514 nm. The red region (622-780 nm) of the visible spectrum of light permits deeper penetration in tissue (Rezzoug *et al.*, 1998) than does other colors of irradiating light. Foscan[®] shows a peak in its fluorescence excitation spectrum at 423 nm. The fluorescence excitation spectrum is the range of light that irradiates the specimen, causing the electrons of the specimen to become stimulated. The fluorescence emission spectrum is the range of light given off from the irradiated sample. The absorption spectrum is the amount of light consumed by the irradiated specimen (see Figure 1.2). Photofrin II[®] is a photosensitizer that is poorly absorbed in the red region of the spectrum. This drug compound has an absorption peak near 630 nm and an excitation peak at 405 nm. A peak absorption in the red region at 648 nm and a peak excitation at 420 nm characterize the drug meso-tetra-hydroxyphenyl-porphyrin. All three photosensitizers have larger absorption peaks in the blue region than in the red region. The reason for using red light and the corresponding smaller peaks is that blue light penetrates weakly into soft tissues. mTHPC has a much larger absorption

at its peak in the red region, as compared to Photofrin II[®] and meso-tetra-hydroxyphenylporphyrin (Ma, *et al.*, 1994), which is seen in Figure 1.3.

1.4 BACK SCATTERED FLUORESCENCE

Luminescence is defined as the emission of light from a material following the initial absorption of energy from an external source – e.g. ultra-violet or high energy radiation. This emission can be categorized as either fluorescence or phosphorescence, depending upon the photon spin. If a spin-allowed transition from a singlet excited state to a singlet ground state occurs, then fluorescence is emitted; whereas if a spin-forbidden transition from a triplet excited state to a singlet ground state occurs, the process is called phosphorescence. Generally, fluorescence is a fast process (less than 10^{-7} s), whereas phosphorescence is regarded as a slower process (greater than 10^{-3} s). Fluorescence arises as a result of the interaction between light and matter. When a photon interacts with a molecule, the molecule may be excited to an upper energy level (see Figure 1.2), provided that the photon is of a wavelength that is short enough (i.e., carries enough energy to bridge the energy gap to the next energy level) (Andersson *et al.*, 1986). Broad fluorescence can result from transitions from excited electronic states to various vibrational and rotational states within the electronic ground state. Figure 1.4 illustrates the fluorescence of HpD, as well as showing the process that leads to the creation of singlet oxygen. Other photosensitizers follow this same process, with the main difference being the use of different wavelengths. In our experiments, a fluorescence emission spectrum was obtained by holding the excited wavelength constant and scanning over the emitted wavelength. For tissues, the relative shape of the fluorescent emission spectrum

is independent of the excitation wavelength. The reason for measuring the fluorescence counts was to determine the relative final concentration of Foscan[®] and to determine optimum times of maximum concentrations in each of the five examined tissues (those being kidney, lung, liver, nasal planum and thyroid).

1.5 CONTRIBUTIONS OF THIS THESIS

Foscan[®] has been well studied for its absorption, fluorescence and emission properties (Ma *et al.*, 1994, Belitchenko *et al.*, 1998, and Grahn *et al.*, 1997). Many studies have also been conducted regarding the application of mTHPC to various cancerous tissues in both animals and humans (Ronn *et al.*, 1995, Ronn *et al.*, 1996, Ronn *et al.*, 1997, Glanzmann *et al.*, 1998). Studies have even been done utilizing the 514.5 nm wavelength of the argon laser (Andrejevic-Blant *et al.*, 1997). This group evaluated mTHPC to determine the optimal drug-light interval for effective photodynamic therapy of early squamous cell carcinomas. Andrejevic-Blant *et al.* utilized ex vivo fluorescence microscopy to quantify time-dependent dye fluorescence in different tissues and tissue compartments. Our in vitro method to determine the concentration of Foscan[®] in different tissues also utilizes a laser-induced fluorescence technique. The purpose of this thesis is to present our results of back scattered fluorescence measurements conducted using an argon laser at 476.5 nm irradiating samples of feline tissues containing mTHPC to determine the optimum times of maximum final concentration and the relative comparison of like tissues.

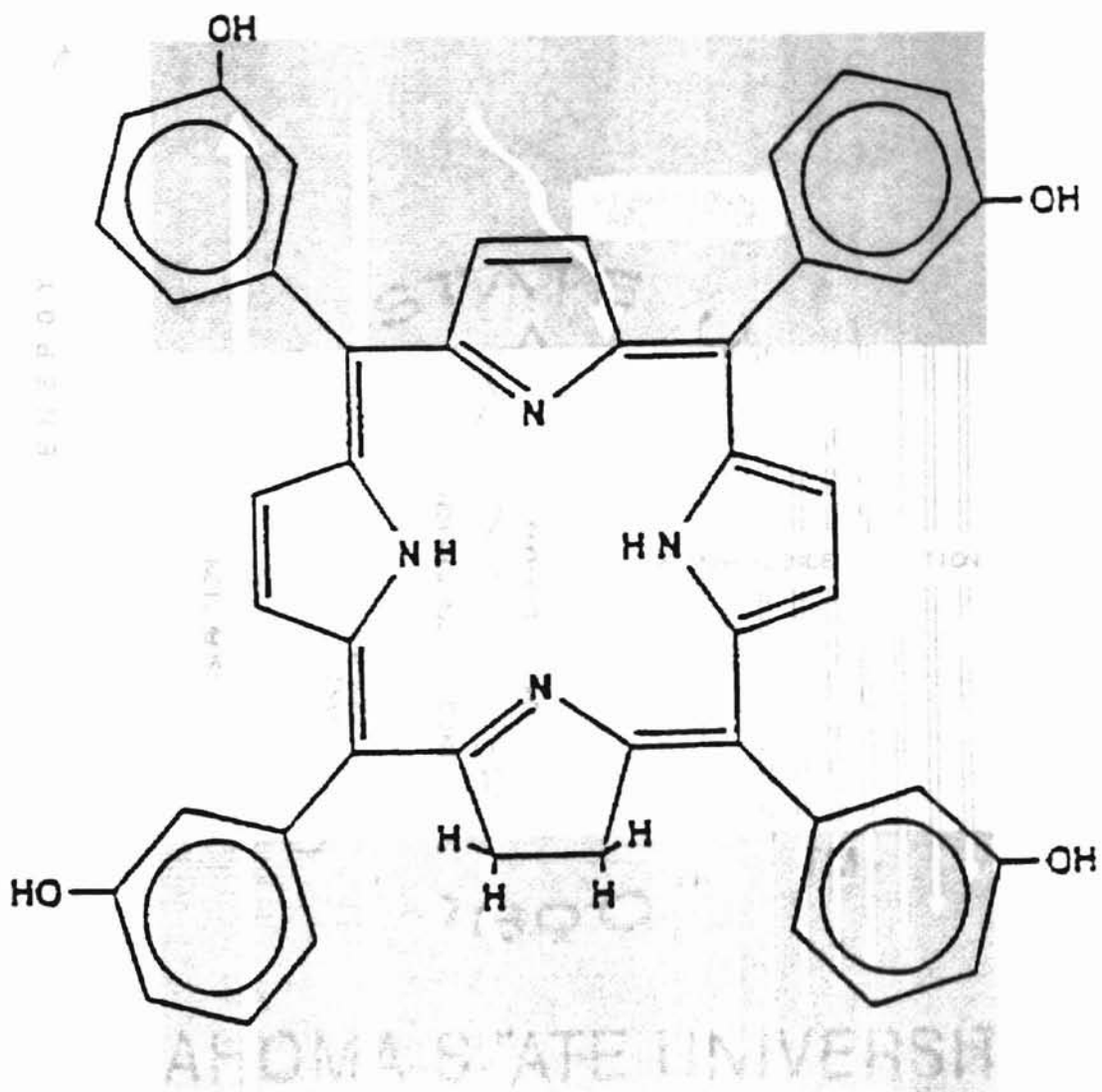


Figure 1.1 Chemical structure for meta-tetra(hydroxyphenyl) chlorin.

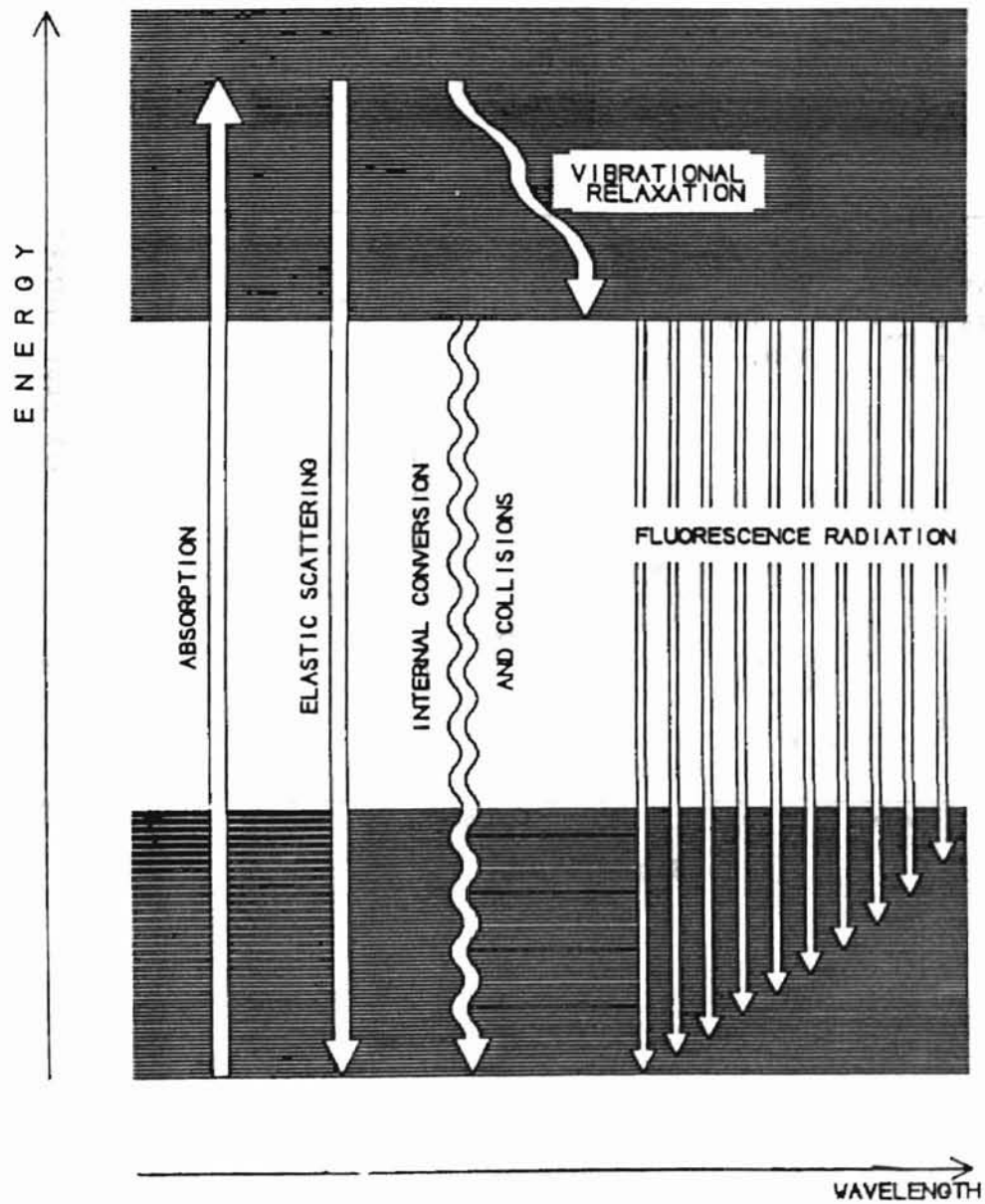


Figure 1.2 Illustration of processes relevant to the energy concepts of fluorescence (courtesy of Andersson *et al.*, 1986).

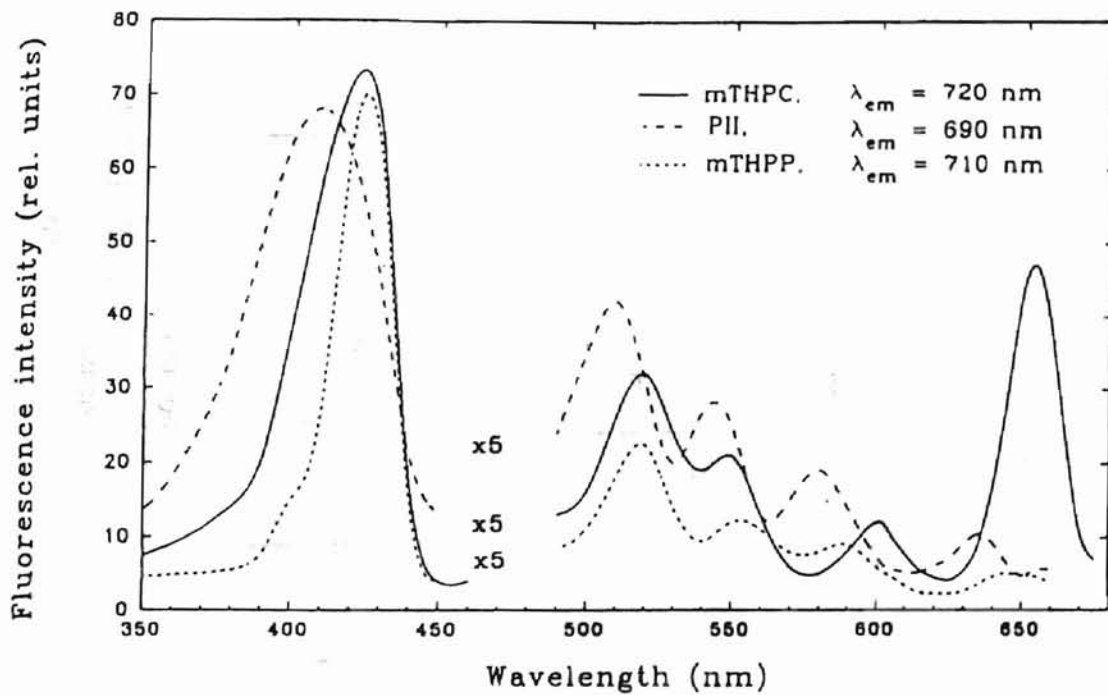


Figure 1.3 Fluorescence-excitation spectra of meta-tetra(hydroxyphenyl) chlorin, Photofrin II[®] and meso-tetra-hydroxyphenyl-porphyrin (courtesy of Ma *et al.*, 1994).

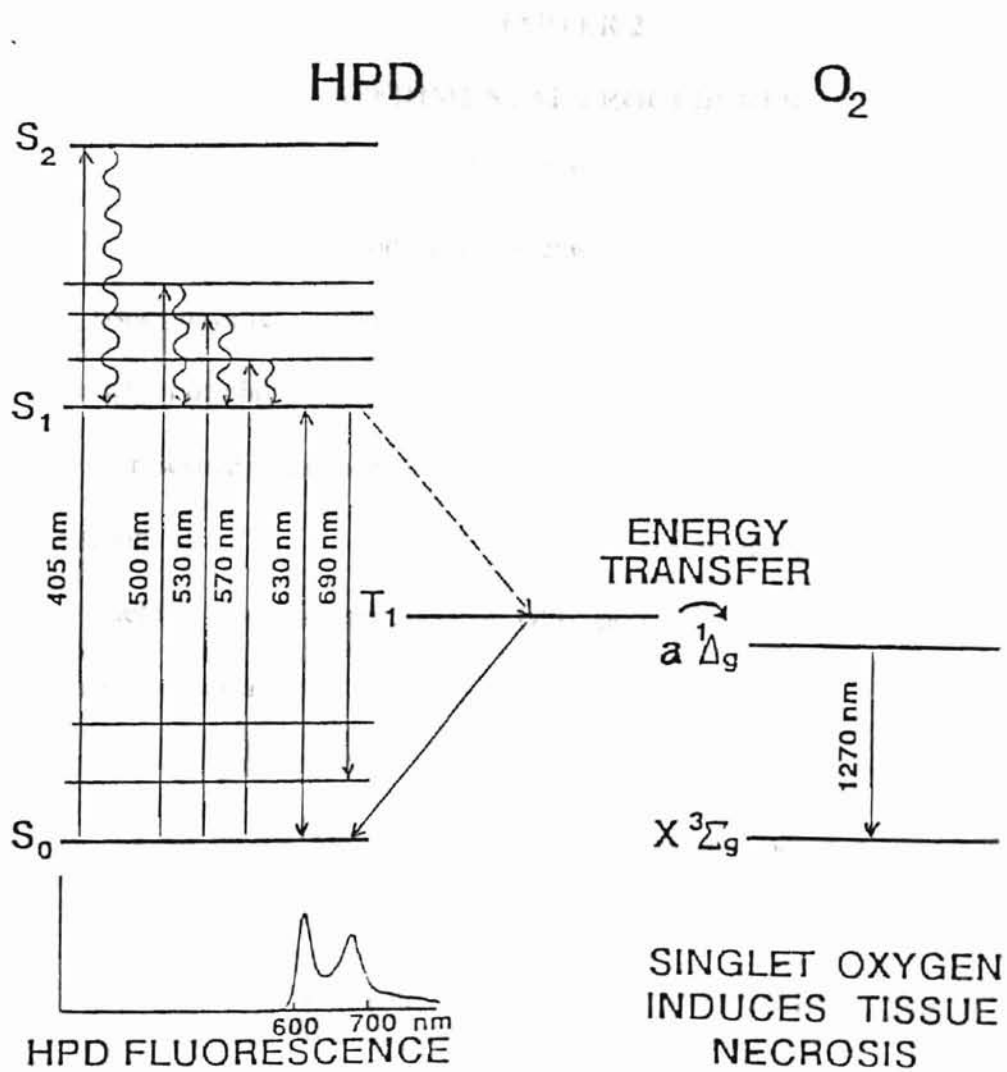


Figure 1.4 The molecular basis for HpD fluorescence and photodynamic action (courtesy of Svanberg, 1989).

CHAPTER 2

EXPERIMENTAL PROCEDURES

2.1 INTRODUCTION

Most fluorescence studies of meta-tetra(hydroxyphenyl) chlorin (mTHPC) induced tissues have relied upon in vitro methods of determining optimal conditions for the introduction of photodynamic therapy. In an in vitro study performed utilizing laser-induced fluorescence, the tissue (Syrian hamster cheek pouch mucosa) was fast frozen in liquid nitrogen by contact with isopentan slush and frozen (Andrejevic-Blant *et al.*, 1997). For feline tissues injected with mTHPC, no studies have been done to date on an in vivo method of measuring the fluorescence counts.

This thesis will report on the back scattered fluorescence of actual sections of Foscan[®] induced, otherwise unadulterated, feline tissue exposed to argon laser light (476.5 nm) as the excitation source. This study is a preliminary step in our laboratory towards the development of an in vivo method for determination of Foscan[®] in feline tissues.

2.2 SAMPLE PREPARATION (ANIMAL)

Cats were obtained through Oklahoma State University Laboratory Animal Resources. Experimental protocol was evaluated and approved by the Oklahoma State University Institutional Animal Care and Use Committee. Seventeen cats averaging

3.5 kg in weight and evenly distributed between males and females were used for the evaluation of Foscan[®]. The drug was slowly injected through an intravenous catheter into each animals' cephalic vein over a period of one to two minutes. Cats were separated into four cohorts. One set of two served as a control (no Foscan[®] was administered). Another array of five was injected with 0.15 mg/kg. A third section of six was given a dose of 0.30 mg/kg. The fourth allotment of four was injected with 0.60 mg/kg. The Foscan[®]-injected animals were sacrificed over a period of time ranging from 24 to 336 hours post-injection. Tables 2.1-2.3 depict the drug concentration and hours after injection before sacrifice of each cat. Animals were housed in a dedicated kennel area illuminated with fluorescent light tubes and shaded natural light. The fluence rate was 1.5 mW/m² for the top bank of cages and 2.9 mW/m² for the bottom bank of cages. The lights were turned on for brief periods of time to perform blood tests and for feeding of the animals. At this time, the fluence rates were 805 mW/m² and 315 mW/m², respectively. The animals were only taken out of their cages for these periodic blood tests (at 0, 1, 6, 24, 48, 72, 96, and 336 hrs post-injection) and necropsy. Necropsies were performed and histopathology was done on all tissues collected, to determine if the Foscan[®] had altered the structure of the tissues. Cats were euthanized with 1.5 ml of Beuthanasia-D[®] (Schering-Plough Animal Health, Irving, TX). Immediately after completion of necropsy, harvested tissues were frozen at -80° C and stored until fluorescence analysis took place. Samples were stored for several months under these conditions.

Upon conducting fluorescence experiments, the tissues were prepared in the following manner. Each tissue was removed from the freezer and cut into thin sections with a number 10 scalpel blade. One section of each tissue was taken for observation, and

the remainder of each tissue was returned to the freezer. The tissue was then placed into a cryotube, and transported from the Boren Veterinary Medical Teaching Hospital to the Physical Sciences Building. Tissues were placed in the freezer section of a refrigerator and brought to a temperature of approximately -5°C while experimental pretests were conducted.

2.3 EXPERIMENTAL SETUP AND SAMPLE PREPARATION

A Spectra-Physics model 2020 argon ion laser was utilized to perform this experiment. The wavelength employed for the exciting of the tissues was 476.5 nm. The laser provided monochromatic light to the specimen. This beam was sent through a neutral density filter to attenuate the power of the laser light. After the laser light passed through the filter, several mirrors directed the light towards the target tissue. The power of the beam measured 5 mW. An Olympus 10X microscopic objective was used to focus the beam onto the tissue, which had previously been placed onto the microscope stage. Tissues were prepared so that the laser light struck the sample as close to a horizontal plane as possible. No illumination of the tissue, other than the excitation light, was present during the recording of the fluorescence data.

The scattered light reflected by the tissue was collected by a lens and passed through a polarization analyzer and polarization scrambler into one of two monochromators of a Jobin-Yvon Ramanor U-1000 micro-macro spectrometer system. Each monochromator features an asymmetric Czerny-Turner mounting with two symmetrical opening slits. Slit sizes, which limit the amount of light allowed to pass into the photomultiplier tube (PMT), were set at 200 μm each. Light exiting the double

monochromator setup was directed into an RCA C31034 PMT. The PMT was cooled to -20°C using a Products for Research thermoelectric cooling unit. The PMT coupled with a preamplifier and discriminator was connected to an IBM PC to record data.

The system was aligned daily to guarantee reproducibility and to insure machine and operator errors were dealt with before samples were exposed to the light of the room, air and the laser. A schematic representation of the irradiation experimental setup is presented in Figure 2.1.

Other parameters that must be accounted for include the time interval between data points (step size) and the range of the emission spectrum. The step size, which determines the number of points taken per scan, was 0.1684 nm, allowing a total of 751 points per scan. The wavelength spectrum emitted from our tissue sample ranged from 588.7 nm to 715.0 nm. Scans lasted approximately 30 minutes. At the end of a given scan, the tissue appeared to be drier than prior to the experiment, primarily due to the exposure of the tissue to the environment of the lab and the thermal heating of the tissue. No charring of the tissue was noticeable under microscopic observation. We attempted to keep the laser power to as low a level as possible in order to prevent the tissue structure from changing and altering the data collection towards the end of each scan.

The software utilized to visualize and record the fluorescence intensity data, on the IBM PC referred to previously, was the Enhanced Program Software version 1.2 from Instruments S.A., Inc. The computer program also compiled the data into ASCII form onto the hard drive of the computer. Data was transported in ASCII form on a floppy disk and imported into and graphed by Sigma-Plot for Windows (version 4.0) on a different IBM PC. Each of the five separate tissues was analyzed using PeakFit (Jandel Scientific

Software, version 4) to determine the shape of the peaks and the background line functions. The results of this analysis will be discussed in Chapter 3.

SPECIMEN NUMBER	TIME BEFORE EUTHANIZATION (hours)
3458	24
3459	48
3463	72
3454	96
3438	96

Table 2.1 Cats and tissue harvesting time for animals injected with 0.15 mg/kg.

SPECIMEN NUMBER	TIME BEFORE EUTHANIZATION (hours)
3449	24
3446	48
3461	72
3460	96
3457	336
3462	336

Table 2.2 Cats and tissue harvesting time for animals injected with 0.30 mg/kg.

SPECIMEN NUMBER	TIME BEFORE EUTHANIZATION (hours)
3464	24
3456	48
3455	72
3453	96

Table 2.3 Cats and tissue harvesting time for animals injected with 0.60 mg/kg.

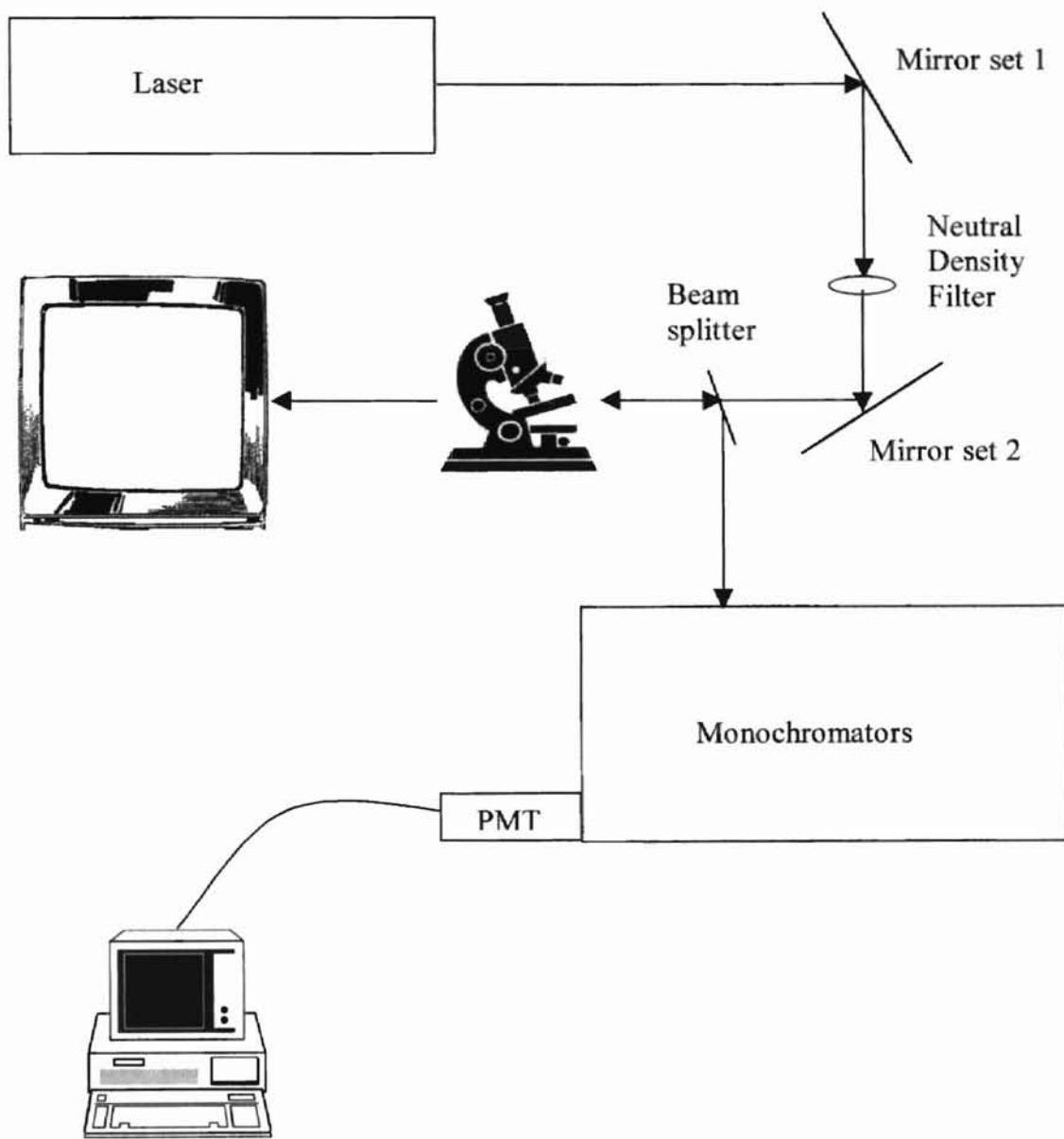


Figure 2.1 Experimental setup.

CHAPTER 3

RESULTS AND DISCUSSION

3.1 INTRODUCTION

Various feline tissues containing Foscan[®] were irradiated with light from an argon laser, and the back scattered fluorescence was measured. The data presented within this chapter utilized an exciting wavelength of 476.5 nm, and the emitted light ranged from 588.7 nm to 715.0 nm. Samples were taken from 17 cats, and five tissues were taken from each cat, for a total of 85 analyzed tissues. It should be noted that cat #3454 escaped from its cage and remained missing for two days. This animal is included in the study, but we are aware that the data that is taken from its tissues could give erroneous data, due to possible uncontrolled exposure to light. The five tissues evaluated were kidney, liver, lung, nasal planum and thyroid. For each respective tissue, the average of the two autofluorescent scans (no Foscan[®]) was subtracted from the fluorescent intensity data, as was the dark count (the contribution to the intensity signal from the machinery involved). For example, for the kidney, the autofluorescence was measured for animals #3445 and #3448. An average was taken, and the dark count of 140 counts was subtracted out (see Figure 3.1). This gave peak structures due only to the Foscan[®] concentration. Figures 3.2-3.23 are of the raw fluorescent intensity data, which include the autofluorescence. The experimental data consists of the fluorescence intensity level (given in arbitrary units) and the emitted wavelength (given in nm) over which the sample was scattered. Figures 3.2 show an

autofluorescence and a fluorescent intensity spectrum for the liver of an animal (injected with 0.60 mg/kg) sacrificed after 24 hours. The fluorescent intensity data was shifted to align the baselines. Tabulated data was measured relative to these baselines. The measuring of the fluorescence intensity level gives us a method of determining relative rankings of dosages and time intervals, in order to discern which of the drug-time combinations is most advantageous. Tables 3.1-3.5 give the values and the statistical deviations of the Foscan[®] induced peaks. The deviations given in these tables arise from the fitting analysis, not from the averaging of several specimens from the same sample tissue.

An example of a normalized graph, which is a graph showing several peak intensities on an autofluorescent background, can be seen in Figure 3.10b.

3.2 KIDNEY DATA ANALYSIS

For animals #3446 (0.30 mg/kg, 48 hours), #3453 (0.60 mg/kg, 96 hours), #3455 (0.60 mg/kg, 72 hours), #3456 (0.60 mg/kg, 48 hours), #3460 (0.30 mg/kg, 96 hours) and #3464 (0.60 mg/kg, 24 hours), large intensity peaks were found. This implies that high levels of Foscan[®] were present. Medium-sized peaks were noted for cats #3449 (0.30 mg/kg, 24 hours), #3457 (0.30 mg/kg, 336 hours), #3458 (0.15 mg/kg, 24 hours), #3459 (0.15 mg/kg, 48 hours) and #3463 (0.15 mg/kg, 72 hours). Small peaks were seen in the scans of animals #3438 (0.15 mg/kg, 96 hours), #3454 (0.15 mg/kg, 96 hours), #3461 (0.30 mg/kg, 72 hours) and #3462 (0.30 mg/kg, 336 hours). Cat #3456 had a peak of more than 700 counts, the largest amplitude for any kidney sample. These data illustrate that this time interval, when combined with this Foscan[®] dosage, will produce maximum

final drug concentration in the kidney. The kidney from cat #3455 also had a high peak intensity, rising approximately 600 counts above the background fluorescence. The peak for this specimen was not as sharp at its maximum intensity as that from cat #3456. The fluorescence analysis showed that the kidney from cat #3453 peaked more than 500 counts above the background fluorescence. Many other kidney samples also gave well-defined peaks. The concentration of 0.60 mg/kg was injected into all three cats whose fluorescence measurements gave the most impressive peaks. It appears that the optimum time will be more than 24 hours after injection of Foscan[®], most likely at 48 hours. Figures 3.3-3.6 plot the fluorescent intensity data, while Table 3.1 gives the fluorescent intensity data for the kidney.

3.3 LIVER DATA ANALYSIS

From the fluorescence analysis, we see that the large peaks were found in the fluorescence measurements of the livers of cats #3453 (0.60 mg/kg, 96 hours), #3455 (0.60 mg/kg, 72 hours), #3456 (0.60 mg/kg, 48 hours), #3458 (0.15 mg/kg, 24 hours) and #3464 (0.60 mg/kg, 24 hours). Medium peaks were noted for animals #3449 (0.30 mg/kg, 24 hours), #3456 (0.30 mg/kg, 96 hours) and #3463 (0.15 mg/kg, 72 hours). Small peaks were noted for samples from cats #3438 (0.15 mg/kg, 96 hours), #3446 (0.30 mg/kg, 48 hours), #3454 (0.15 mg/kg, 96 hours), #3459 (0.15 mg/kg, 48 hours), and #3461 (0.30 mg/kg, 72 hours). Minimal peaks were noted for animals #3457 (0.30 mg/kg, 336 hours) and #3462 (0.30 mg/kg, 336 hours). An intensity peak, registering almost 600 counts at its apex, was noted for cat #3464. The peak was very sharp, as it had very small standard deviation for its full width half maximum (FWHM). The liver from cat #3456 had a well-

defined peak rising almost 425 counts above the fluorescence background. This peak was not as large as that of the previous specimen, nor was it as sharp. The fluorescent intensity for cat #3455 had a peak, which, at its apex, was not very sharp. The peak value for the intensity registered 400 counts. Again, the drug concentration level of 0.60 mg/kg was prevalent among the tissues that had the largest values of peak intensity. These three concentration-time interval combinations (0.60 mg/kg at 24, 48 and 72 hours) appear to be the most advantageous for application of irradiating light. Foscan[®] is a hard drug, nearly completely eliminated in the liver, so we expected to see high values for the peak intensities for this tissue. The largest peak intensity was found in a 24-hour cat, suggesting that the highest level of Foscan[®] can be found near this time. Other 24-hour cats gave medium level peak intensities. Table 3.2 gives the statistical data for the various combinations of drugs and times for the liver. Figures 3.7-3.10 show the fluorescence of each liver specimen. Figure 3.10b shows the normalized emission spectra of liver injected with 0.60 mg/kg of mTHPC.

3.4 LUNG DATA ANALYSIS

High drug concentrations can be assumed for cats #3446 (0.30 mg/kg, 48 hours), #3449 (0.30 mg/kg, 24 hours), #3456 (0.60 mg/kg, 48 hours), #3458 (0.15 mg/kg, 24 hours) and #3464 (0.60 mg/kg, 24 hours) due to their large peaks. Low concentrations were found for cats #3453 (0.60 mg/kg, 96 hours), #3454 (0.15 mg/kg, 96 hours), #3455 (0.60 mg/kg, 72 hours), #3459 (0.15 mg/kg, 48 hours), #3456 (0.30 mg/kg, 96 hours) and #3463 (0.15 mg/kg, 72 hours). Minimal concentrations of mTHPC were found in animals #3438 (0.15 mg/kg, 96 hours), #3457 (0.30 mg/kg, 336 hours), #3461 (0.30 mg/kg, 72

hours) and #3462 (0.30 mg/kg, 336 hours). A very large peak was found for the lung of cat #3464. This peak's amplitude measured around 1175 counts. Animal #3449 was found to have an amplitude near 450 counts. Cat #3458 was found to have the third largest intensity peak for the lung. The fluorescence analysis showed an amplitude rising almost 400 counts above the background fluorescence. In this tissue, the time interval seemed to be the more important parameter for large amplitudes of intensity, as opposed to the initial dosage. The three samples with the largest peaks all were necropsied 24 hours after being injected with Foscan[®]. The lung, being another highly vascularized tissue, had high concentration levels of mTHPC, in comparison to other tissues. This was expected due to an increased blood flow to these areas through more extensive capillary networks. Figures 3.11-3.14 give the fluorescent intensity plots of the lung samples, while Table 3.3 gives the raw statistical data.

3.5 NASAL PLANUM DATA ANALYSIS

The only large intensity peak for the nasal planum was from cat #3455 (0.60 mg/kg, 72 hours). Small intensity peaks were found in animals #3453 (0.60 mg/kg, 96 hours), #3456 (0.60 mg/kg, 48 hours), #3461 (0.30 mg/kg, 72 hours) and #3464 (0.60 mg/kg, 24 hours), while only minimal peaks were noted in any of the remaining specimens. Cat #3455 had an intensity peaking around 300 counts. The peak for this measurement was sharp and well-defined. Animal #3456 had a distinguished peak rising above the autofluorescence surrounding 652 nm. The peak reached an amplitude of approximately 150 counts. Cat #3461 was found to have an intensity peak of almost 125 counts. The time interval between introduction of mTHPC and introduction of laser light

will probably be important for the nasal planum. Somewhere between 48 and 72 hours will give an optimal time to utilize the largest concentration of Foscan[®], as can be seen from the time intervals of the three largest intensity peaks. Figures 3.15-3.18 show the fluorescence and autofluorescence of each nasal planum specimen. Table 3.4 gives the statistical values for all of the investigated nasal planums. For this tissue, time and initial drug concentration appear equally important.

3.6 THYROID DATA ANALYSIS

Large peaks were seen in the fluorescence data for cats #3455 (0.60 mg/kg, 72 hours) and #3456 (0.60 mg/kg, 48 hours). A medium peak was seen for animal #3464 (0.60 mg/kg, 24 hours). Cats #3453 (0.60 mg/kg, 96 hours) and #3463 (0.15 mg/kg, 72 hours) had small intensity peaks, while all other animals had fluorescence data that showed only minimal amplitudes. The thyroid from the fluorescence data of animal #3456 had an amplitude of 400 counts. This peak was well-defined and sharply tipped. This was the best drug-time combination choice for the thyroid gland to be photosensitized. Cat #3455 showed a strong peak in its fluorescence scan as well. The fluorescent intensity amplitude measured 300 counts. Cat #3464 showed a peak rising 250 counts above the autofluorescence. The only concentration of drug that can claim to alter the fluorescence properties of the thyroid was 0.60 mg/kg. The thyroid gland is not as vascularized as kidneys, livers and lungs are, and it does not have peaks near the strength or shape of those tissues that have an extensive vascular system. Larger values for the peak intensity were found at stages of time later than 24 hours. For this tissue, drug dosage is much more important than time interval, but the time interval still shows

that a period of two to three days will permit maximal performance of the injected photosensitizer. The intensity data for the thyroid are displayed in Table 3.5 and plotted in Figures 3.19-3.22.

3.7 DISCUSSION

3.7.1 INTRODUCTION

All the results included in this chapter have been modified on their respective graphs to allow comparison with similarly dosed tissues. Peak shapes or heights have not been altered; only numeric shifting on the fluorescent intensity axis has been performed. The determination of the relative peak height for each sample and the optimal time for largest drug concentration are the basis of this study. The figures give a relationship between peak height and background fluorescence that illustrate the optimum time of maximum photosensitizer concentration. For the most part, the height of the intensities increases as the dosage increases; however, the increase is non-linear.

Several tissues were reexamined to ensure that the experimental results remained fairly consistent throughout the entire data taking process. Examples have been included in Tables 3.1, 3.2 and 3.4 to show the reproducibility of our experiment. The percent differences were 3.0% for kidney (Table 3.1), 2.6% for liver (Table 3.2) and 1.2% for nasal planum (Table 3.4).

Statistical analysis was performed on each sample tissue to determine peak shapes and the form of the background fluorescence functions. Tables 3.1-3.5 summarize all the parameter statistics (fluorescence signal amplitude, center of peak and FWHM of the peak). These statistics take into account a common autofluorescence that has not been

utilized for the plotting of the various fluorescence data. All tissue peaks were of a Gaussian lineshape. The autofluorescence was best defined by a quadratic function ($y=a_0+a_1x+a_2x^2$) for most tissues, although a few backgrounds (primarily of the thyroid) were more closely resembled by a cubic function ($y=a_0+a_1x+a_2x^2+a_3x^3$).

Figure 3.23 shows the plot of the maximum fluorescent intensity versus the time of necropsy for all dosages for kidney specimens.

3.7.2 LONG ISLAND JEWISH MEDICAL CENTER

Finding a large peak does not mean that its dosage time interval is most conducive to PDT. It is possible that this dosage could detrimentally impact most of the surrounding, healthy tissue.

A group led by Dr. Avigdor Ronn at the Long Island Jewish Medical Center analyzed samples from the same tissues as those presented here (Ronn, unpublished data). The samples utilized to record their data were pulverized, combined with dimethyl sulfoxide and centrifuged. The supernatant from tissue extraction was excited at 420 nm spectrofluorometrically over an emission range of 600-700 nm. The method used by this group has been well documented in their experiments on Foscan[®] treated dog, rabbit, rat and human tissues (Ronn *et al.*, 1997).

Although the analyzation methods differ (our method measures fluorescent intensity counts and Dr. Ronn's measures drug concentration), we can see that relative specimen ranks are almost the same. Intensity measurements can be influenced by factors other than the photosensitizer. Effects of concentration of oxygen, water, metal compounds and other fluorescing compounds in the body need to be duly considered.

Most differences were in the numerical placement of higher concentrations to lower concentrations, but nearly all these samples were in the same classification of high, medium or low concentration. Exact matches cannot be expected due to the complexities of animal tissue and the heterogeneity of the examined tissue. These inabilities forced us to acknowledge that the intensity measurements may differ from assay to assay, since different fluorescent compounds will give differing fluorescent intensities (Benson *et al.*, 1979). It was also noted that concentration variability existed between species and between individuals within a single species (Ronn *et al.*, 1997). Two biopsies of the same organ can differ, causing various levels of the drug to be present in the same tissue. None of the tissues differed drastically from the experimental data Dr. Ronn found. The intensities of samples were found to be very similar in many cases.

I concur with Dr. Ronn's resolution that the more vascularized tissues probably have a larger concentration of mTHPC than those tissues that had less blood supplied to them. I have found that the largest fluorescence intensities were primarily found for tissues coming from animals that were injected with 0.60 mg/kg of Foscan[®].

CAT NUMBER	DOSAGE (mg/kg) / TIME (hrs)	AMPLITUDE (a.u.)	CENTER (nm)	FWHM (nm)
3438	0.15 / 96	124±4	653.0±0.2	11.5±0.5
3446	0.30 / 48	330±10	652.7±0.2	15.8±0.6
3449	0.30 / 24	267±20	653.0±0.4	10.9±1.0
3453	0.60 / 96	535±15	652.7±0.2	12.9±0.4
3454	0.15 / 96	153±15	651.8±0.6	13.0±1.5
3455	0.60 / 72	617±13	652.4±0.1	13.3±0.3
3456	0.60 / 48	733±7	653.0±0.1	12.3±0.1
3457	0.30 / 336	289±13	652.7±0.3	13.2±0.7
3458	0.15 / 24	215±6	652.3±0.1	10.0±0.4
3459	0.15 / 48	205±13	652.7±0.4	12.1±0.9
3460	0.30 / 96	302±12	653.0±0.2	10.3±0.5
3461	0.30 / 72	197±14	653.0±0.5	14.5±1.2
3462	0.30 / 336	123±12	651.8±0.6	12.7±1.5
3463	0.15 / 72	260±12	652.4±0.3	13.9±0.8
3464	0.60 / 24	386±16	652.4±0.3	12.7±0.7
3464*	0.60 / 24	409±12	653.0±0.2	14.5±0.5

Table 3.1 PeakFit statistical analysis data for feline kidney (* indicates tissue sample examined to ensure reproducibility).

CAT NUMBER	DOSAGE (mg/kg) / TIME (hrs)	AMPLITUDE (a.u.)	CENTER (nm)	FWHM (nm)
3438	0.15 / 96	140±4	652.7±0.2	12.7±0.4
3446	0.30 / 48	150±4	652.4±0.2	13.9±0.5
3449	0.30 / 24	290±6	652.7±0.1	12.1±0.3
3453	0.60 / 96	352±11	652.7±0.2	14.5±0.5
3454	0.15 / 96	154±8	652.7±0.4	15.7±0.9
3455	0.60 / 72	407±10	653.0±0.2	13.9±0.4
3456	0.60 / 48	371±7	653.0±0.1	13.3±0.3
3456*	0.60 / 48	352±5	653.6±0.1	12.7±0.2
3457	0.30 / 336	16±11	652.7±1.0	3.2±2.5
3458	0.15 / 24	424±10	652.7±0.2	13.3±0.4
3459	0.15 / 48	187±6	652.4±0.2	12.1±0.4
3460	0.30 / 96	236±6	652.7±0.2	14.5±0.5
3461	0.30 / 72	198±8	653.0±0.3	16.3±0.8
3462	0.30 / 336	5±8	653.6±3.1	4.2±7.5
3463	0.15 / 72	231±9	654.2±0.3	15.7±0.8
3464	0.60 / 24	572±7	652.7±0.1	13.3±0.2

Table 3.2 PeakFit statistical analysis data for feline liver (* indicates tissue sample examined to ensure reproducibility).

CAT NUMBER	DOSAGE (mg/kg) / TIME (hrs)	AMPLITUDE (a.u.)	CENTER (nm)	FWHM (nm)
3438	0.15 / 96	83±8	653.0±0.8	17.8±2.0
3446	0.30 / 48	375±8	652.7±0.2	15.1±0.4
3449	0.30 / 24	462±6	653.0±0.1	14.5±0.2
3453	0.60 / 96	114±8	652.7±0.5	15.1±1.3
3454	0.15 / 96	139±6	652.7±0.3	13.9±0.8
3455	0.60 / 72	188±6	654.0±0.2	13.5±0.5
3456	0.60 / 48	343±9	652.4±0.2	15.7±0.5
3457	0.30 / 336	36±6	657.3±0.5	6.0±1.1
3458	0.15 / 24	389±9	652.4±0.2	15.1±0.4
3459	0.15 / 48	183±5	652.7±0.2	15.1±0.5
3460	0.30 / 96	125±8	652.4±0.3	9.7±0.7
3461	0.30 / 72	81±4	654.9±0.4	17.0±0.9
3462	0.30 / 336	33±6	651.2±1.4	16.3±3.6
3463	0.15 / 72	156±4	652.7±0.2	12.5±0.4
3464	0.60 / 24	1179±10	652.7±0.1	14.5±0.2

Table 3.3 PeakFit statistical analysis data for feline lung.

CAT NUMBER	DOSAGE (mg/kg) / TIME (hrs)	AMPLITUDE (a.u.)	CENTER (nm)	FWHM (nm)
3438	0.15 / 96	95±15	653.0±1.0	12.7±2.5
3446	0.30 / 48	44±8	654.5±0.4	4.2±0.9
3449	0.30 / 24	33±10	653.6±0.4	2.5±0.9
3453	0.60 / 96	107±20	651.2±1.3	14.5±3.3
3454	0.15 / 96	38±10	653.3±0.2	19.9±6.5
3455	0.60 / 72	304±8	653.3±0.2	13.3±0.4
3455*	0.60 / 72	311±8	653.6±0.2	12.7±0.4
3456	0.60 / 48	152±5	652.1±2.5	11.5±0.5
3457	0.30 / 336	41±7	660.3±2.0	31.4±6.7
3458	0.15 / 24	48±16	654.4±0.3	1.7±10.7
3459	0.15 / 48	67±10	651.8±1.4	24.2±4.4
3460	0.30 / 96	56±14	653.0±0.6	11.5±3.5
3461	0.30 / 72	117±10	653.3±1.4	14.5±1.5
3462	0.30 / 336	58±13	651.2±1.4	13.1±3.5
3463	0.15 / 72	38±11	651.8±1.5	10.9±3.6
3464	0.60 / 24	110±10	652.7±0.4	8.5±0.9

Table 3.4 PeakFit statistical analysis data for feline nasal planum (* indicates tissue sample examined to ensure reproducibility).

CAT NUMBER	DOSAGE (mg/kg) / TIME (hrs)	AMPLITUDE (a.u.)	CENTER (nm)	FWHM (nm)
3438	0.15 / 96	41±16	652.1±3.1	16.9±7.4
3446	0.30 / 48	152±12	652.9±0.3	13.2±1.3
3449	0.30 / 24	40±6	650.8±0.2	3.2±0.6
3453	0.60 / 96	105±20	652.4±1.0	10.9±2.4
3454	0.15 / 96	14±5	654.0±0.3	1.9±0.8
3455	0.60 / 72	302±14	652.7±0.3	14.4±0.8
3456	0.60 / 48	400±8	652.7±0.1	12.7±0.3
3457	0.30 / 336	75±27	651.2±3.2	18.7±8.1
3458	0.15 / 24	47±6	652.7±1.5	23.6±3.9
3459	0.15 / 48	30±28	663.2±2.0	9.9±8.8
3460	0.30 / 96	62±17	651.8±2.3	17.5±5.7
3461	0.30 / 72	74±14	653.0±0.5	7.6±1.9
3462	0.30 / 336	61±21	650.3±5.6	33.5±15.0
3463	0.15 / 72	100±29	653.0±2.1	14.5±4.9
3464	0.60 / 24	250±26	652.7±0.7	13.3±1.6

Table 3.5 PeakFit statistical analysis data for feline thyroid.

CATS: Foscan® (0.15 mg/kg)

Final Concentration µg/kg

TISSUE	24 hours	48 hours	72 hours	96 hours (escapee)	96 hours
Kidney	0.625	0.7	0.933	0.594	0.721
Liver	2.952	1.373	0.846	0.848	0.954
Lung	2.184	0.408	0.647	0.217	0.217
Nasal Planum	0.067	0.12	0.19	0.19	0.23
Thyroid	0.233	0.159	0.239	0.175	0.122

CATS: Foscan® (0.30 mg/kg)

Final Concentration µg/kg

TISSUE	24 hours	48 hours	72 hours	96 hours	336 hours (#3457)	336 hours (#3462)
Kidney	1.071	1.367	0.668	1.378	1.219	1.187
Liver	3.021	1.961	1.06	1.325	0.398	0.438
Lung	2.756	1.431	1.378	1.007	0.26	0.141
Nasal Planum	0.138	0.228	0.164	0.191	0.053	0.127
Thyroid	0.259	0.198	0.244	0.307	0.148	0.148

CATS: Foscan® (0.60 mg/kg)

Final Concentration µg/kg

TISSUE	24 hours	48 hours	72 hours	96 hours
Kidney	2.502	2.459	1.251	1.961
Liver	4.346	4.618	1.855	1.802
Lung	4.399	4.717	1.961	1.166
Nasal Planum	0.149	0.557	0.228	0.477
Thyroid	0.382	0.382	0.456	0.657

Table 3.6 Results of biodistribution study of Foscan® performed by Dr. Ronn's group at Long Island Jewish Medical Center.

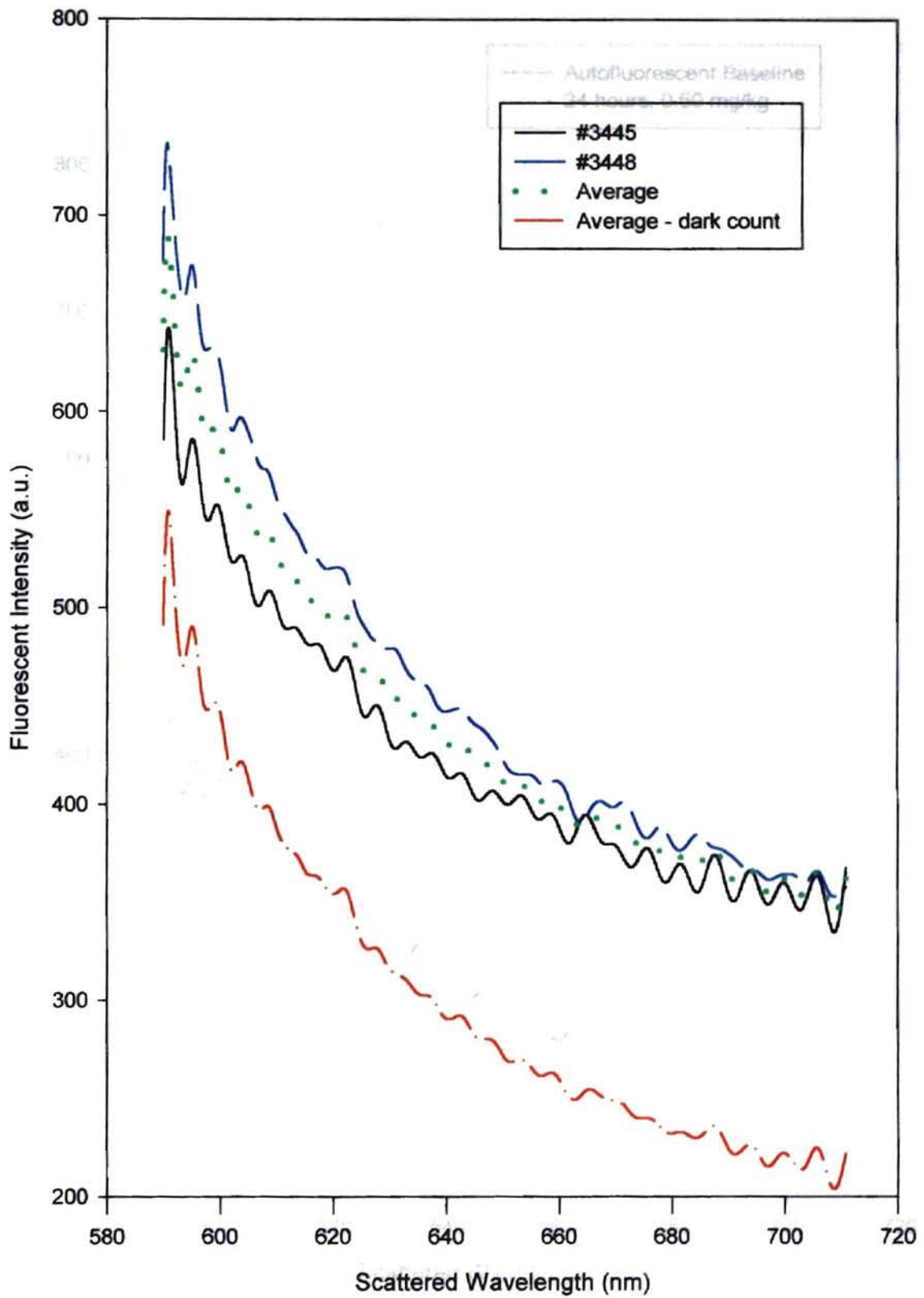


Figure 3.1 Example of method used to determine calculation of autofluorescence (kidney).

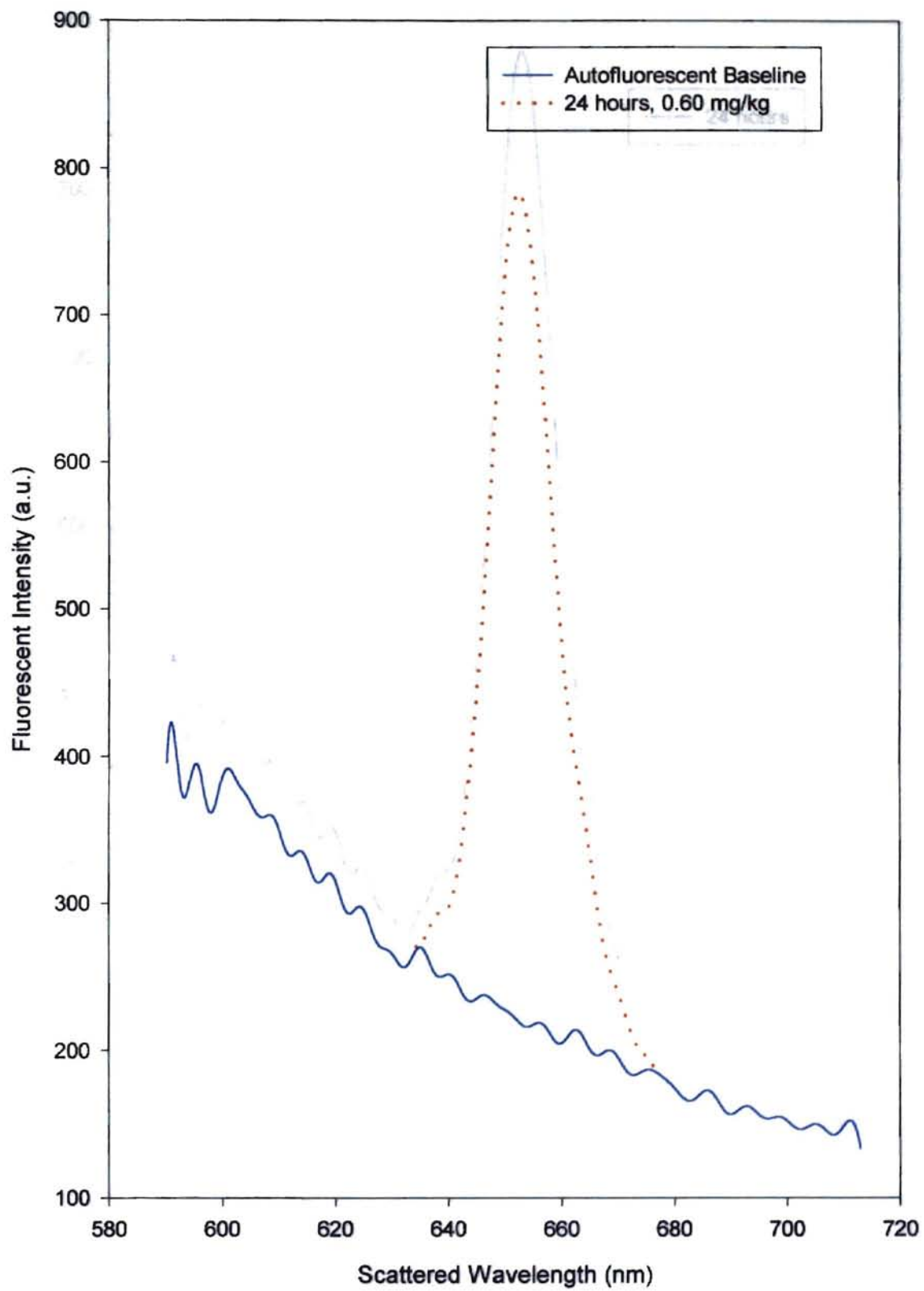


Figure 3.2a Fitting demonstration for peak, FWHM and center analysis of liver data (24 hours, 0.60 mg/kg).

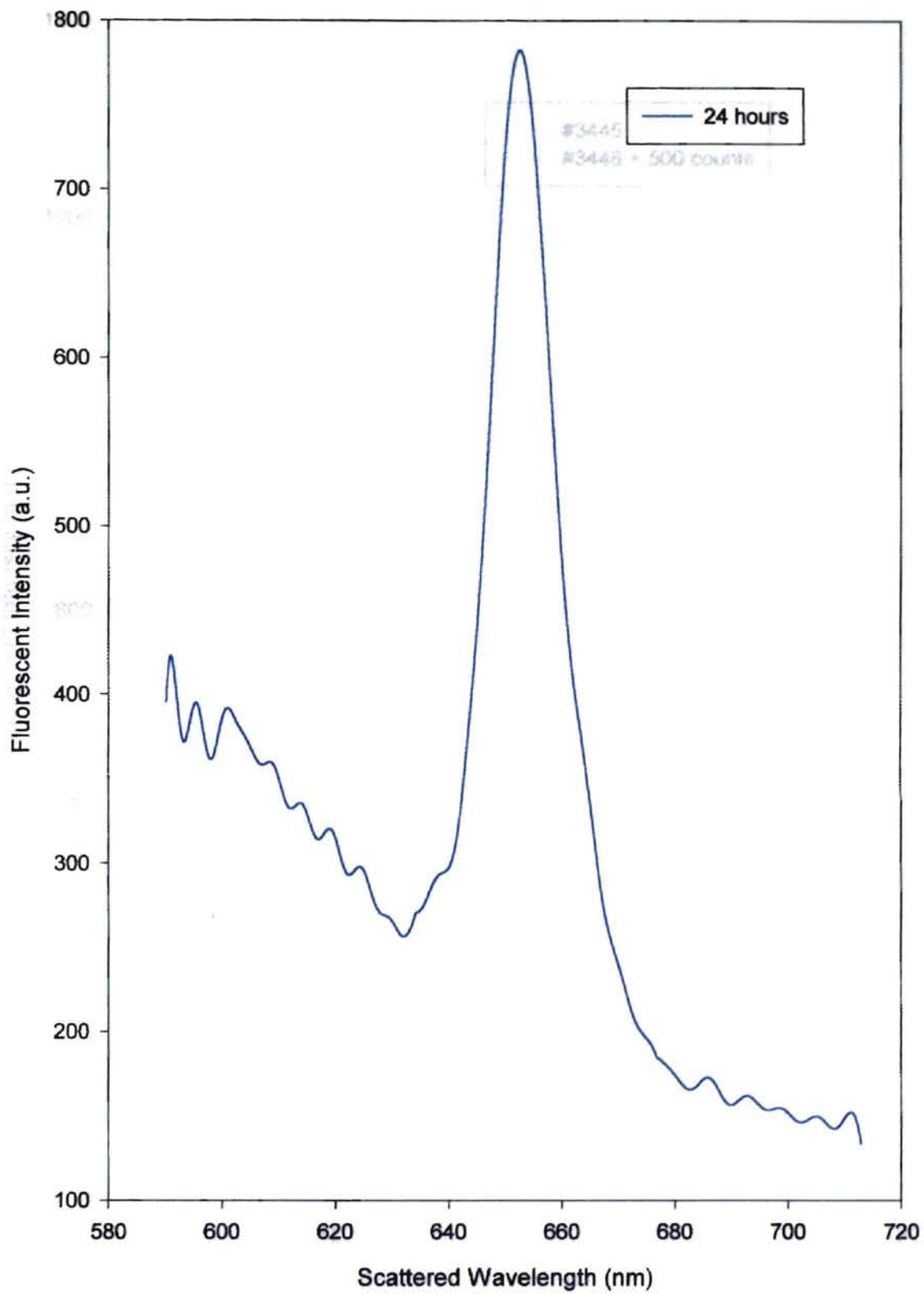


Figure 3.2b Fitting demonstration for peak, FWHM and center analysis of liver data (24 hours, 0.60 mg/kg).

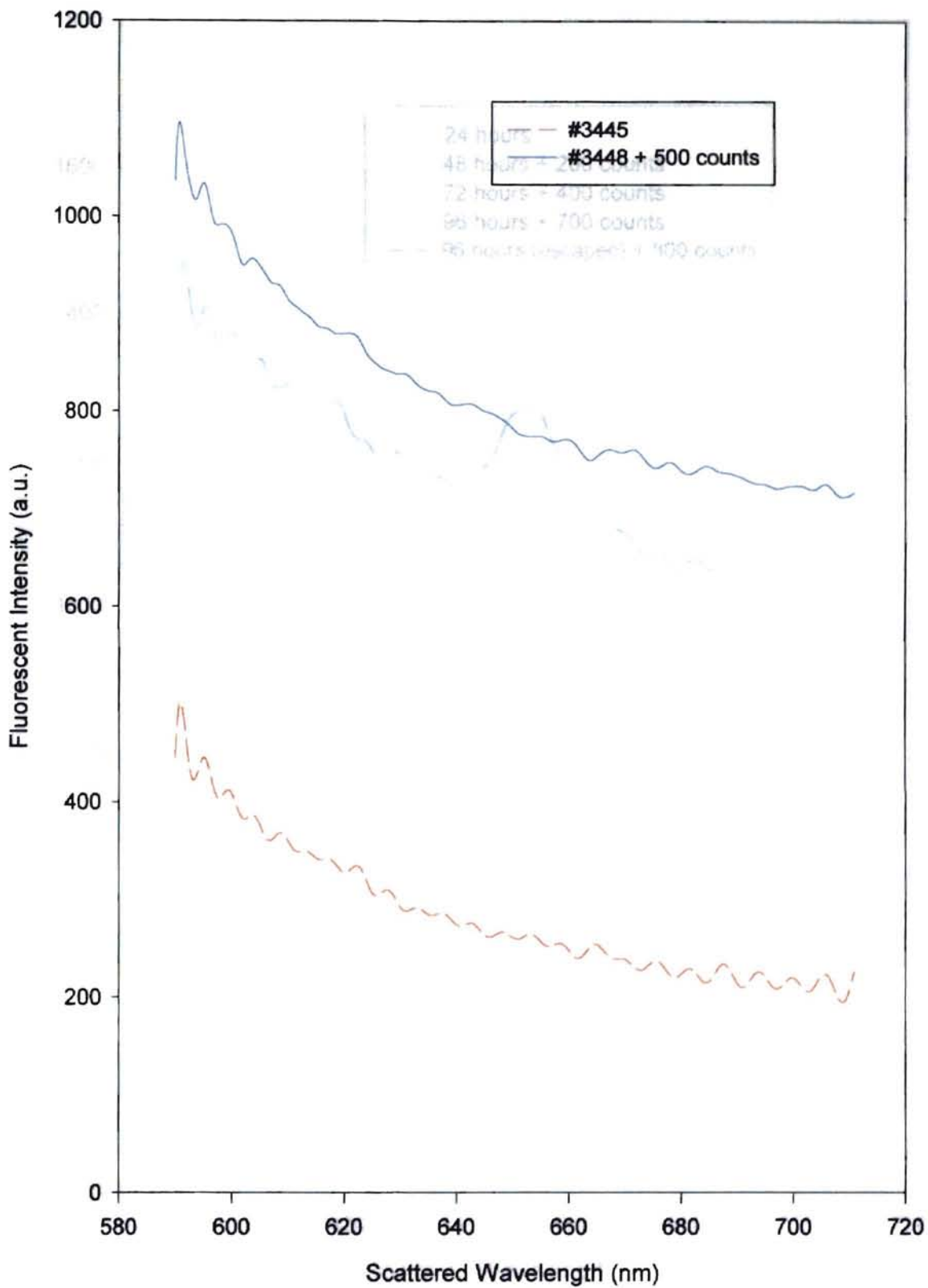


Figure 3.3 Emission spectra of kidney not injected with Foscan®.

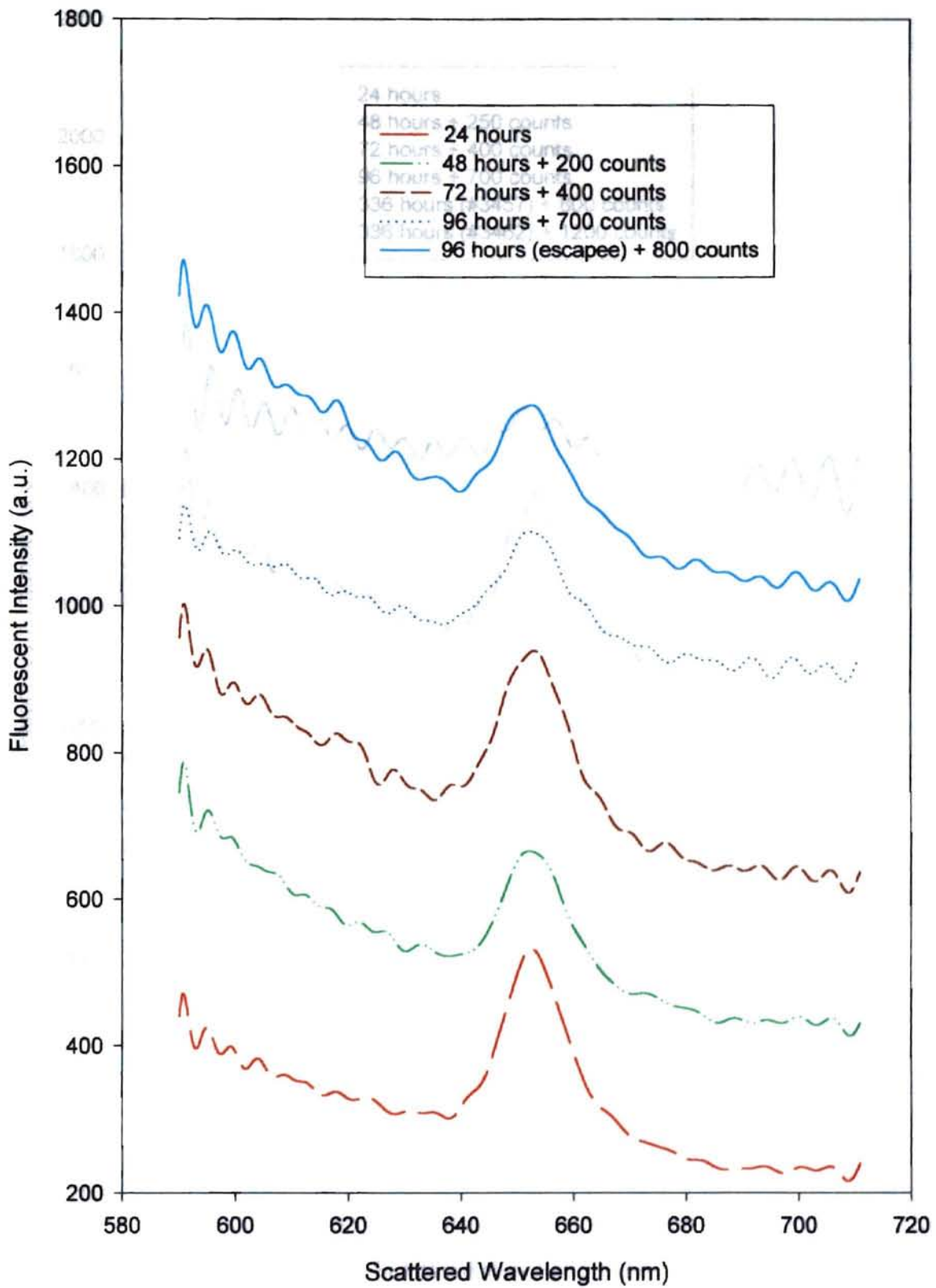


Figure 3.4 Emission spectra of kidney injected with 0.15 mg/kg of Foscan®.

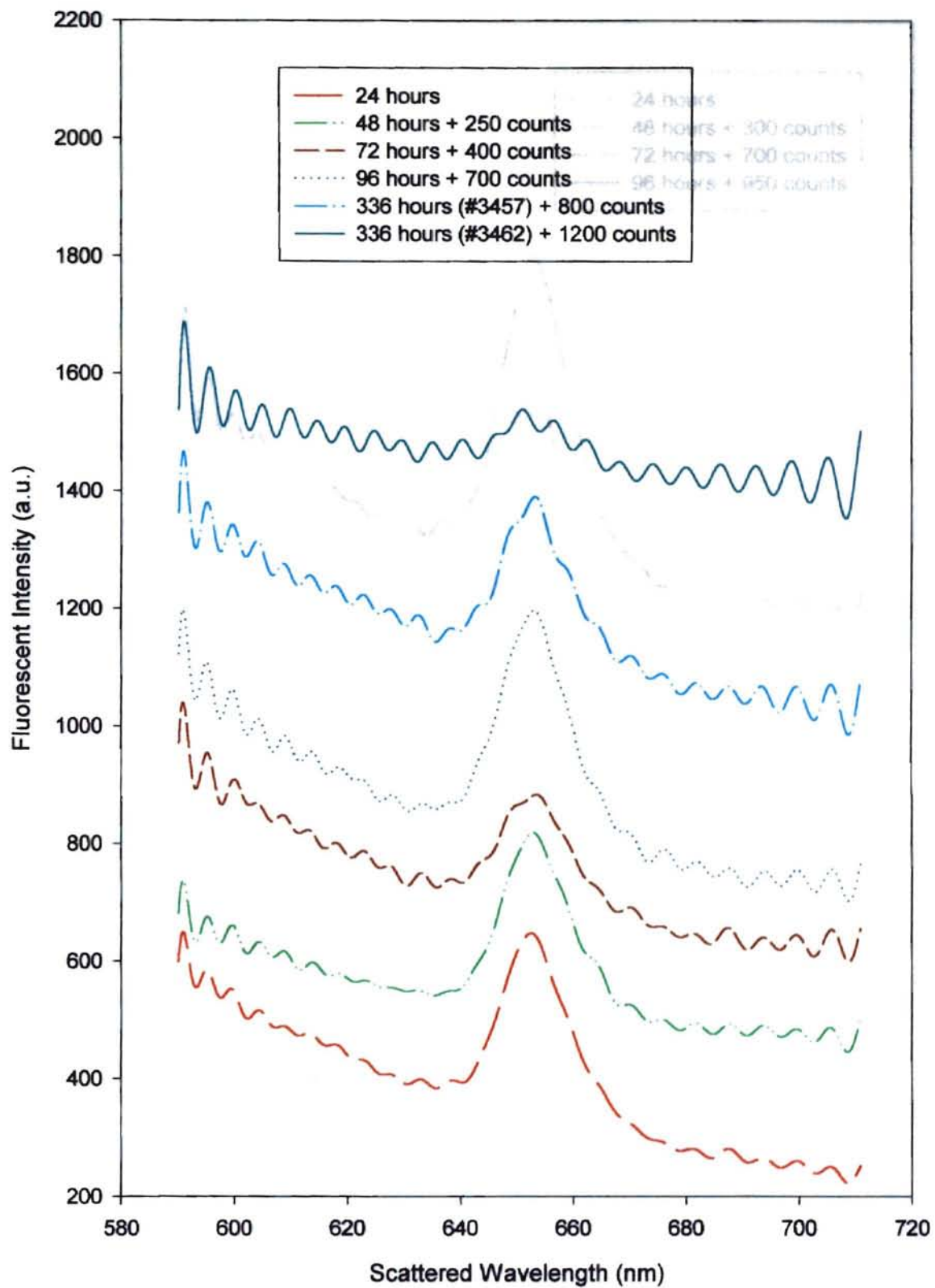


Figure 3.5 Emission spectra of kidney injected with 0.30 mg/kg of Foscan®.

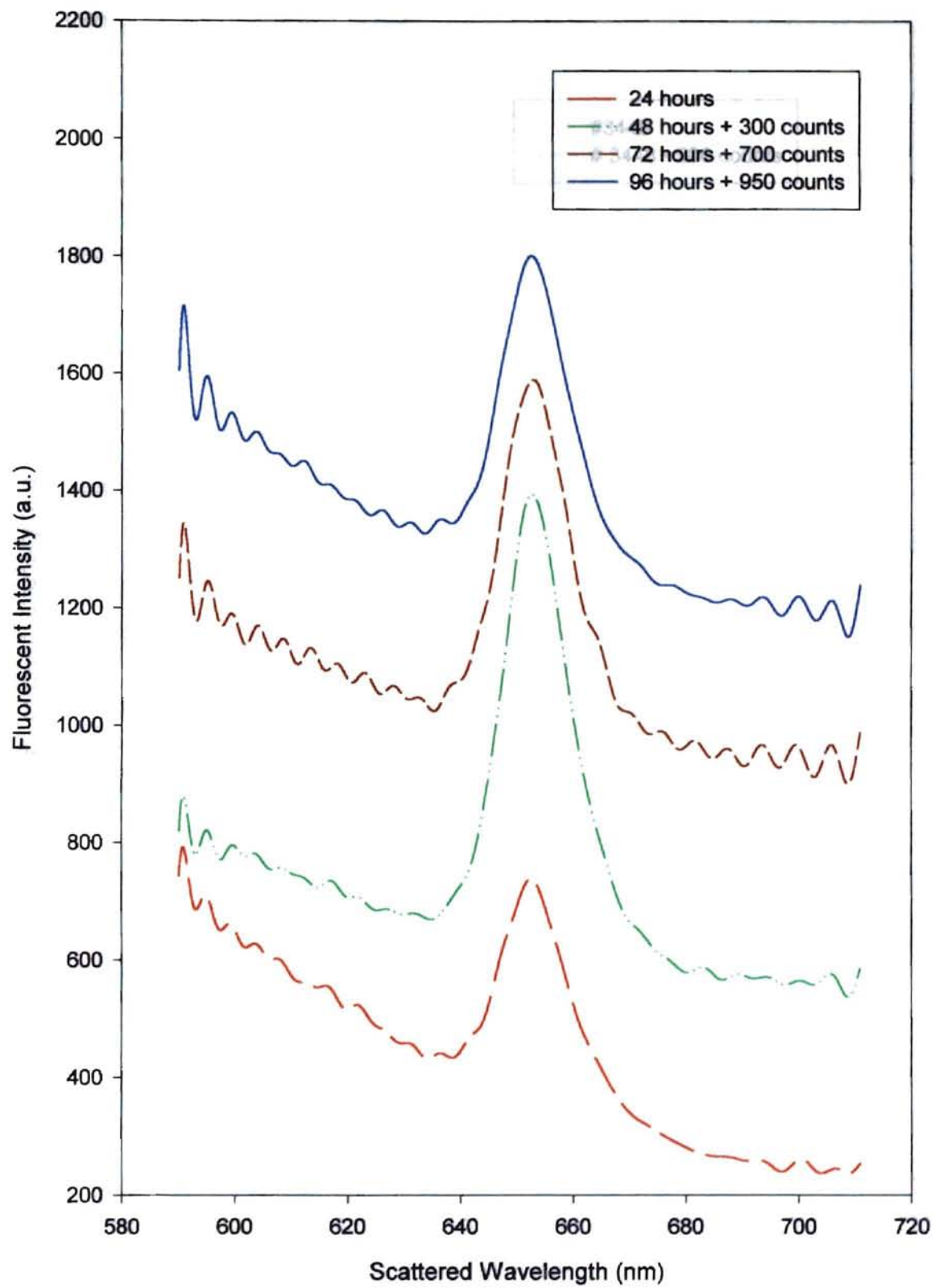


Figure 3.6 Emission spectra of kidney injected with 0.60 mg/kg of Foscan®.

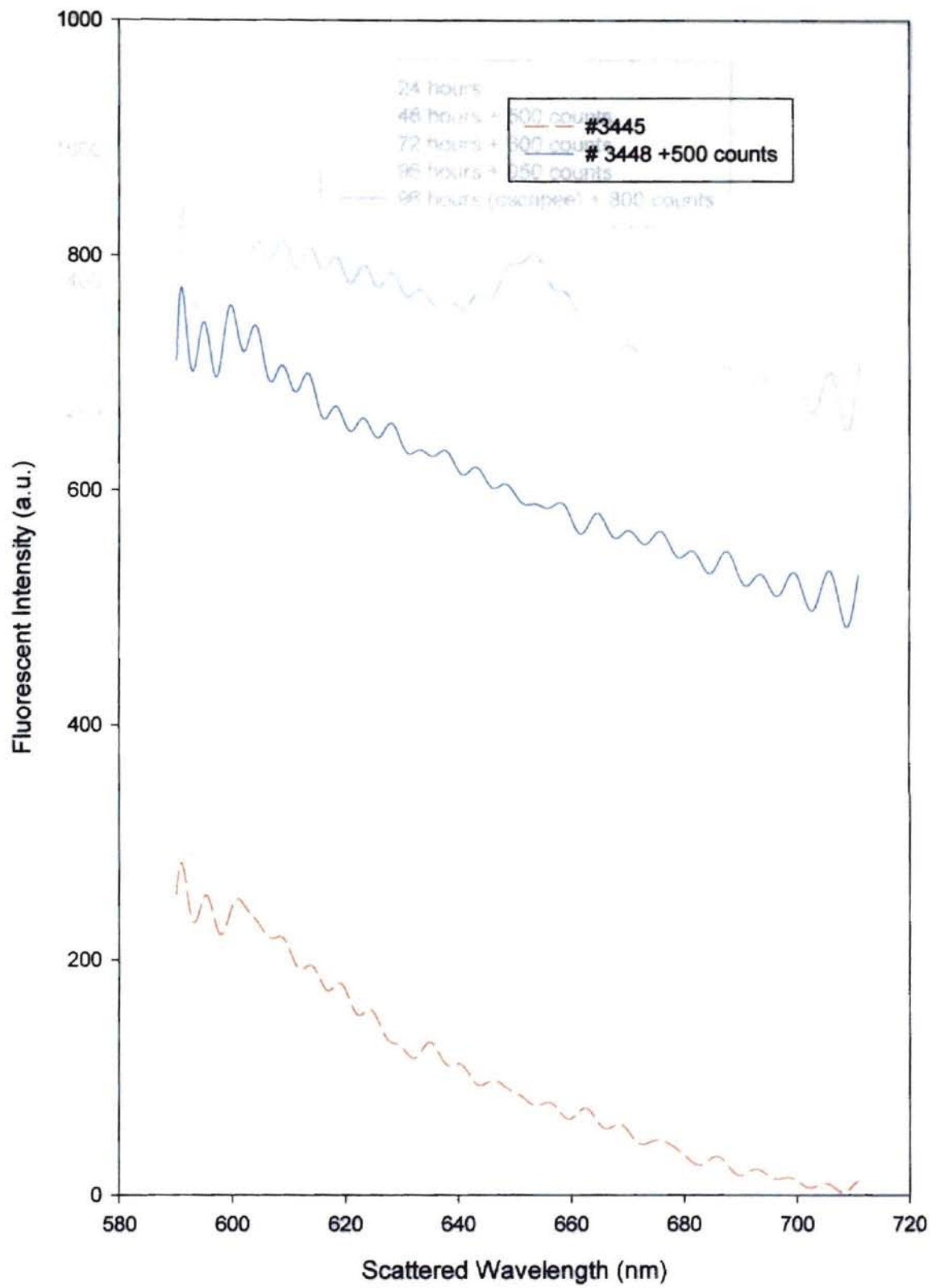


Figure 3.7 Emission spectra of liver not injected with Foscan®.

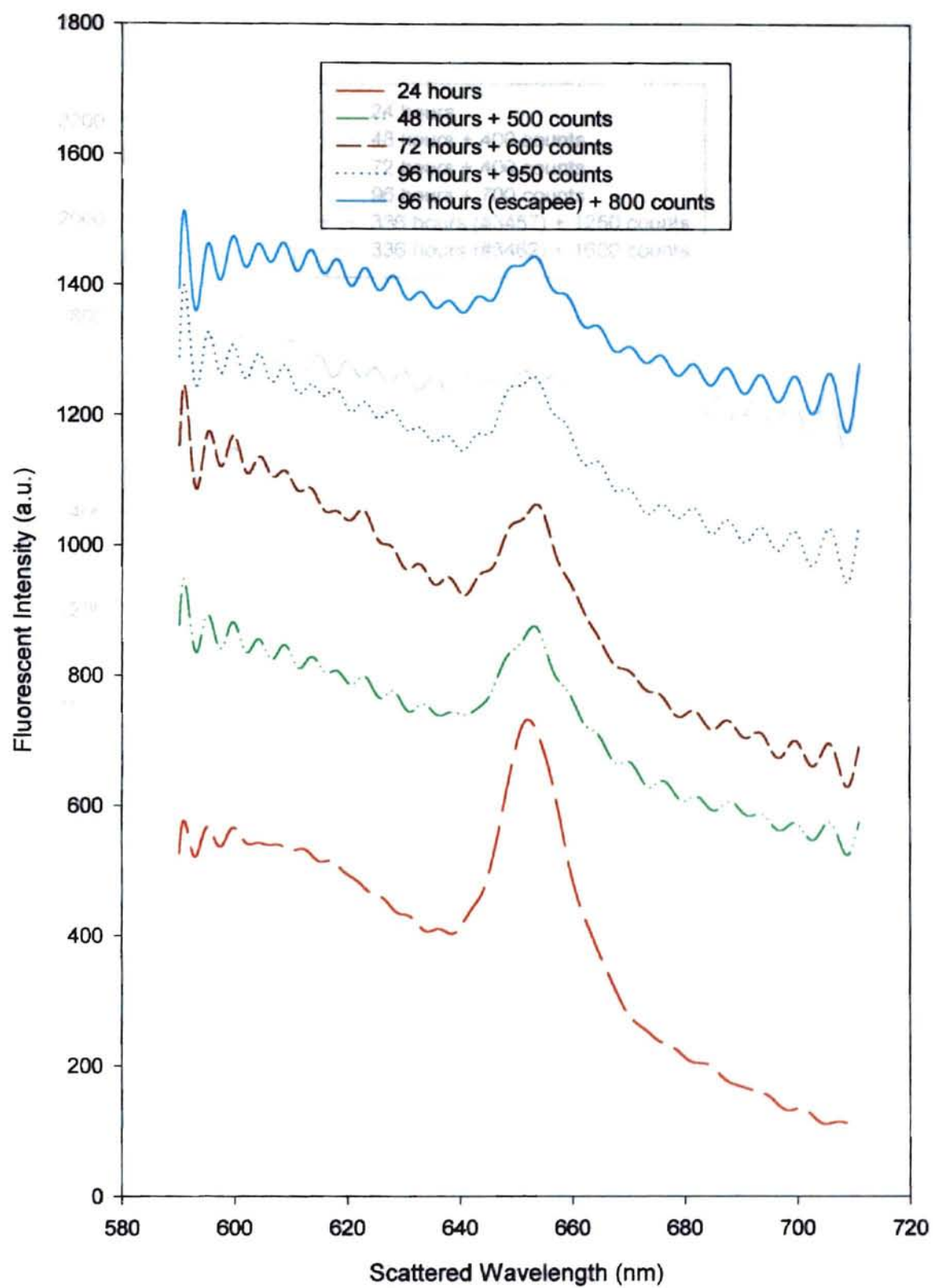


Figure 3.8 Emission spectra of liver injected with 0.15 mg/kg of Foscan®.

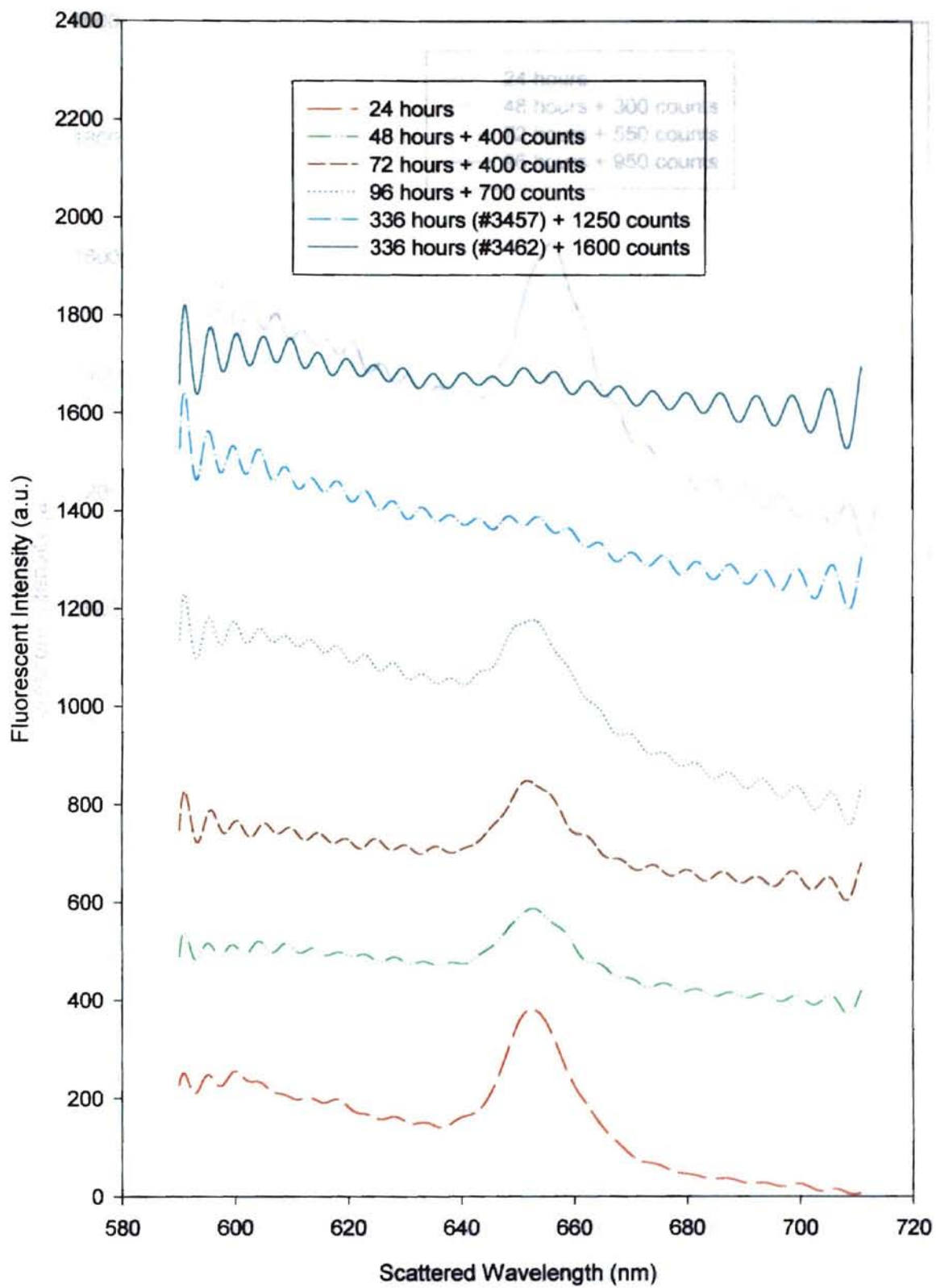


Figure 3.9 Emission spectra of liver injected with 0.30 mg/kg of Foscan®.

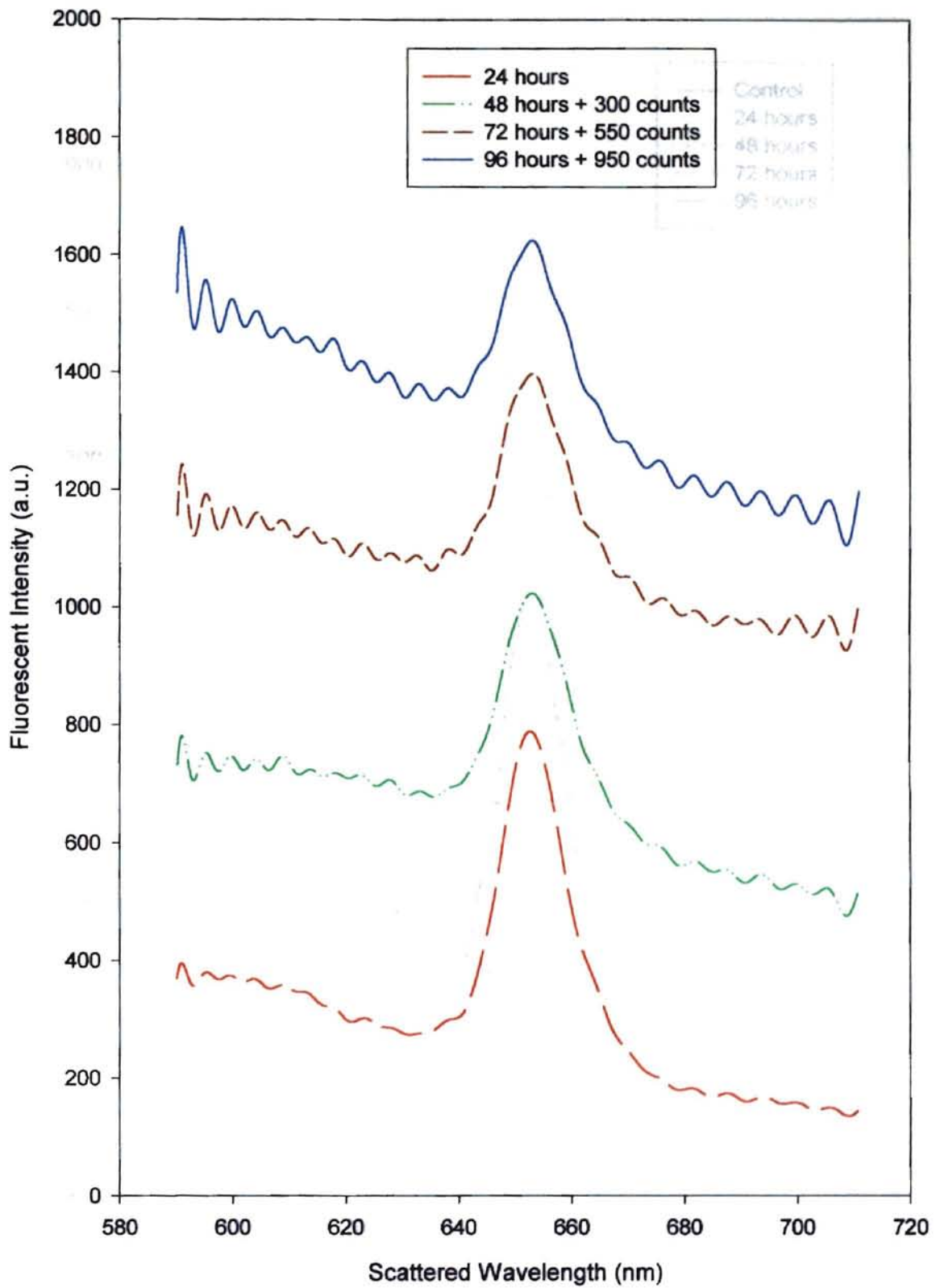


Figure 3.10a Emission spectra of liver injected with 0.60 mg/kg of Foscan®.

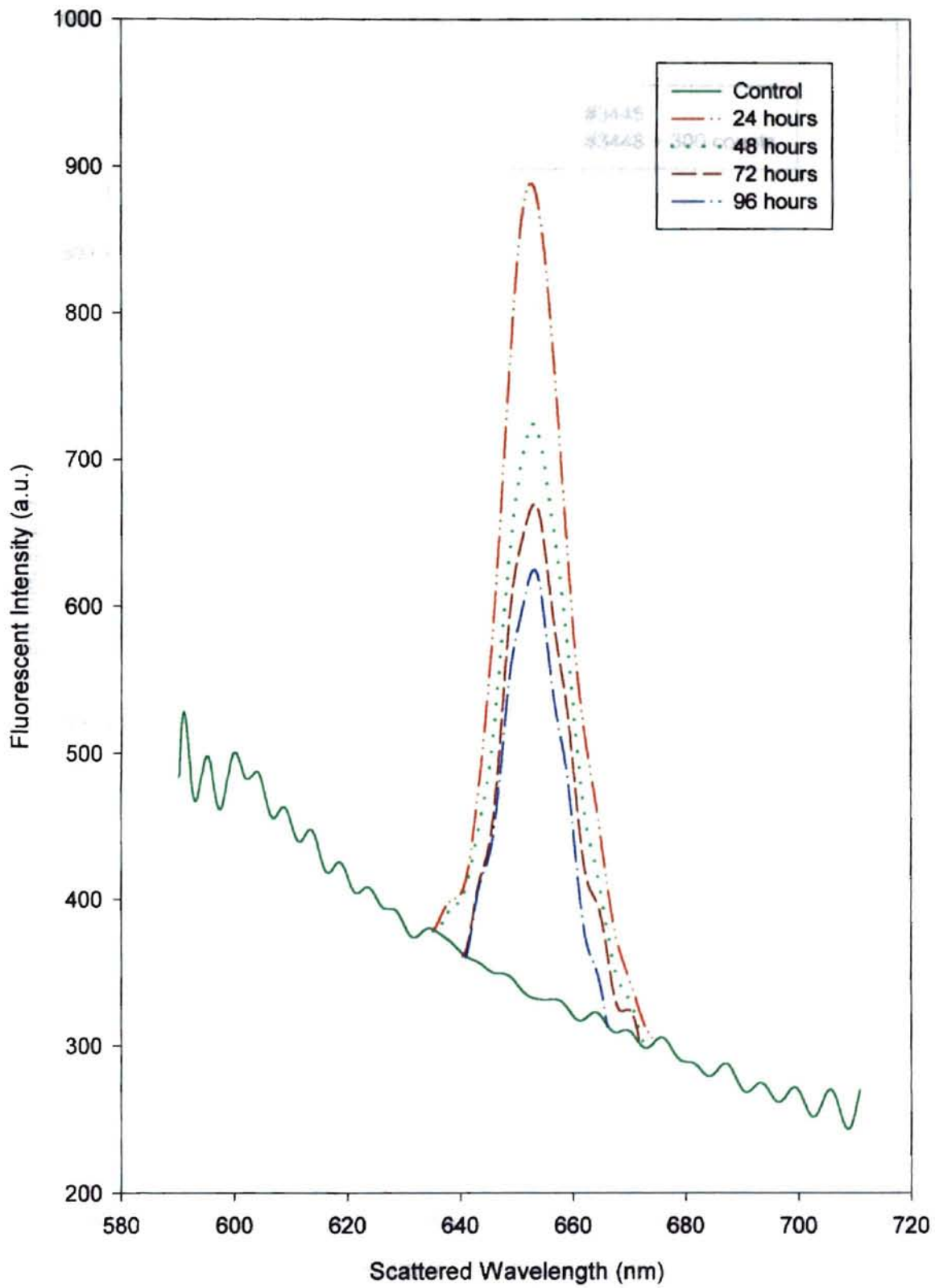


Figure 3.10b Normalized emission spectra of liver injected with 0.60 mg/kg of Foscan®.

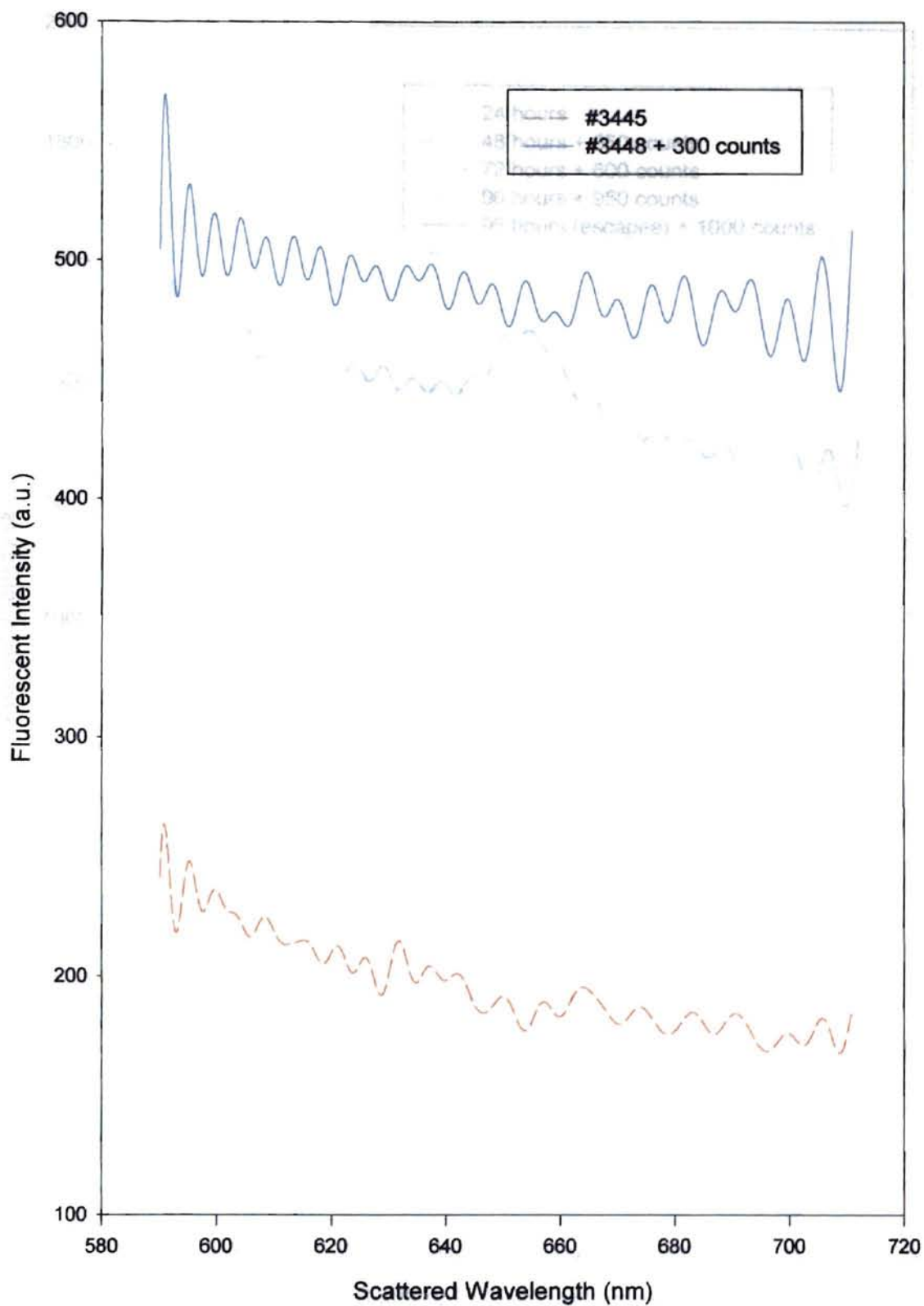


Figure 3.11 Emission spectra of lung not injected with Foscan®.

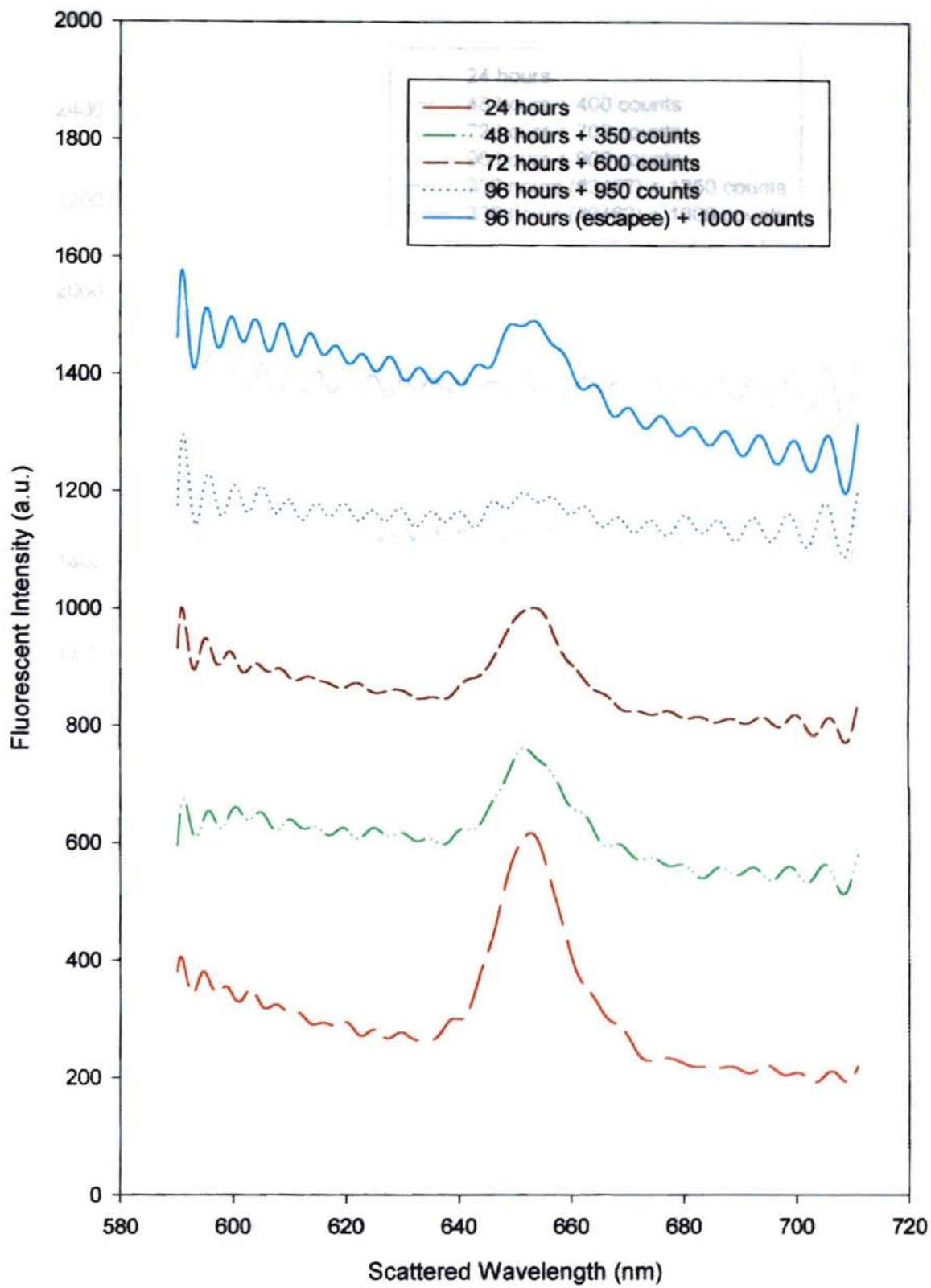


Figure 3.12 Emission spectra of lung injected with 0.15 mg/kg of Foscan®.

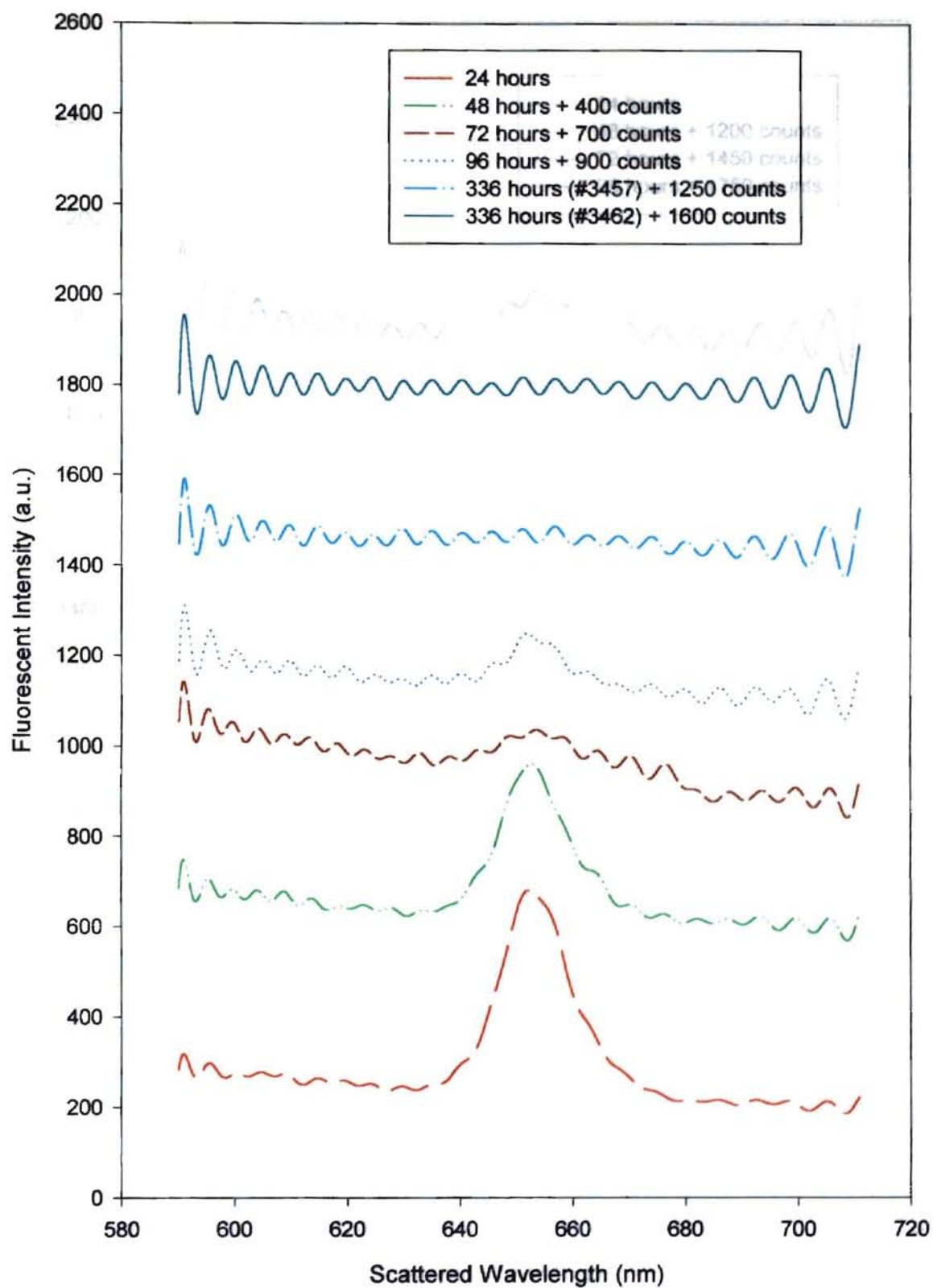


Figure 3.13 Emission spectra of lung injected with 0.30 mg/kg of Foscan[®].

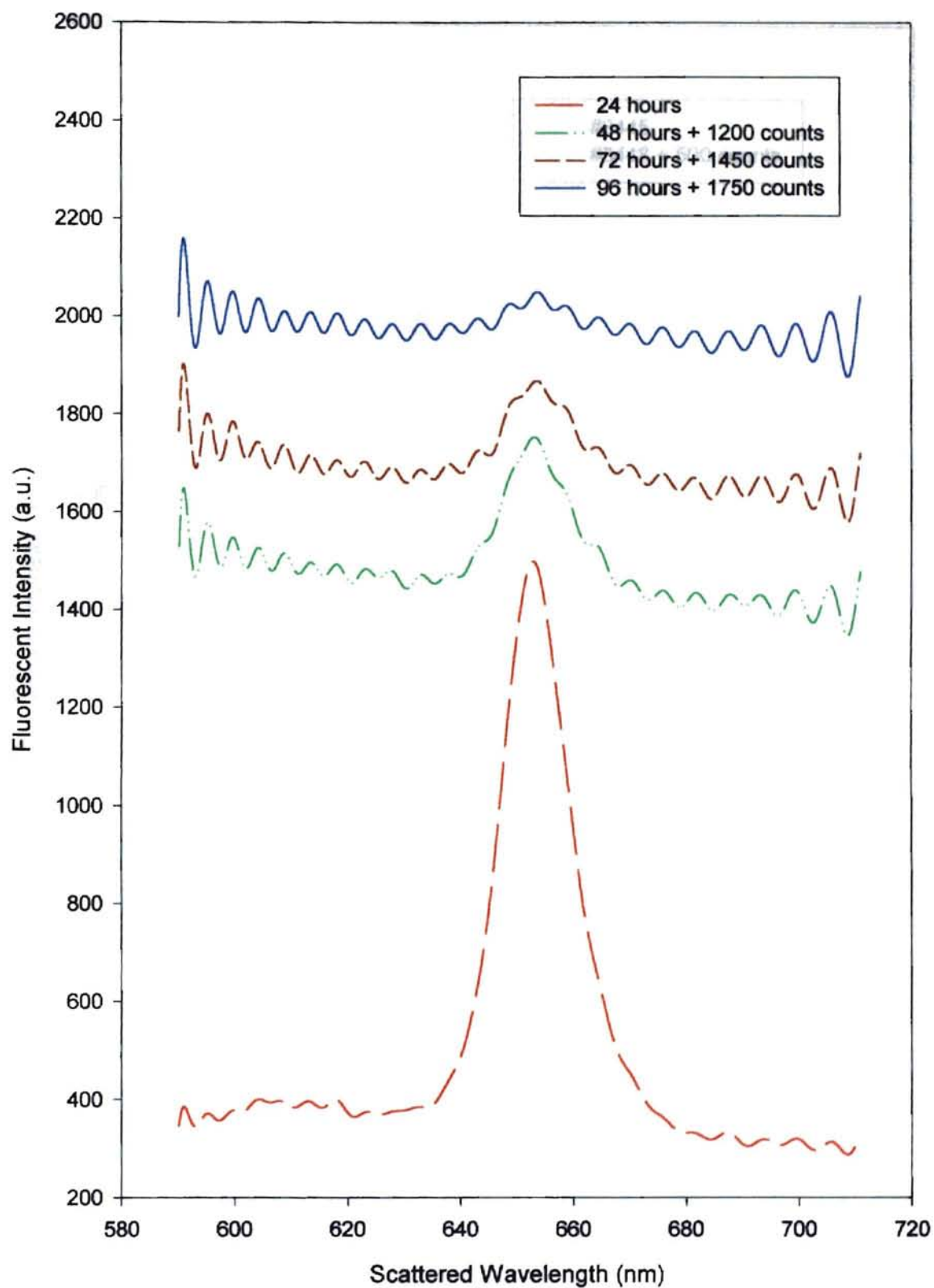


Figure 3.14 Emission spectra of lung injected with 0.60 mg/kg of Foscan®.

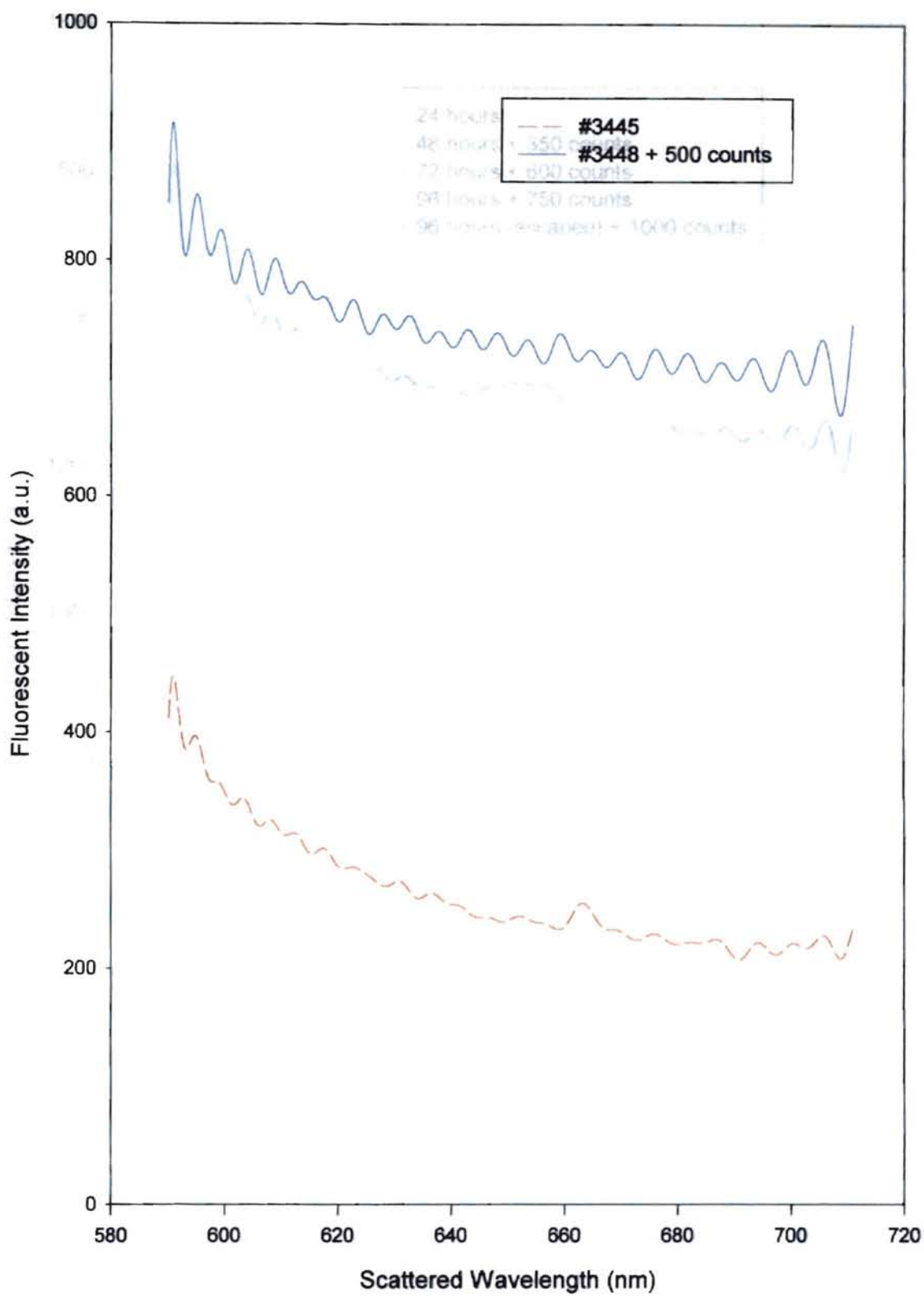


Figure 3.15 Emission spectra of nasal planum not injected with Foscan®.

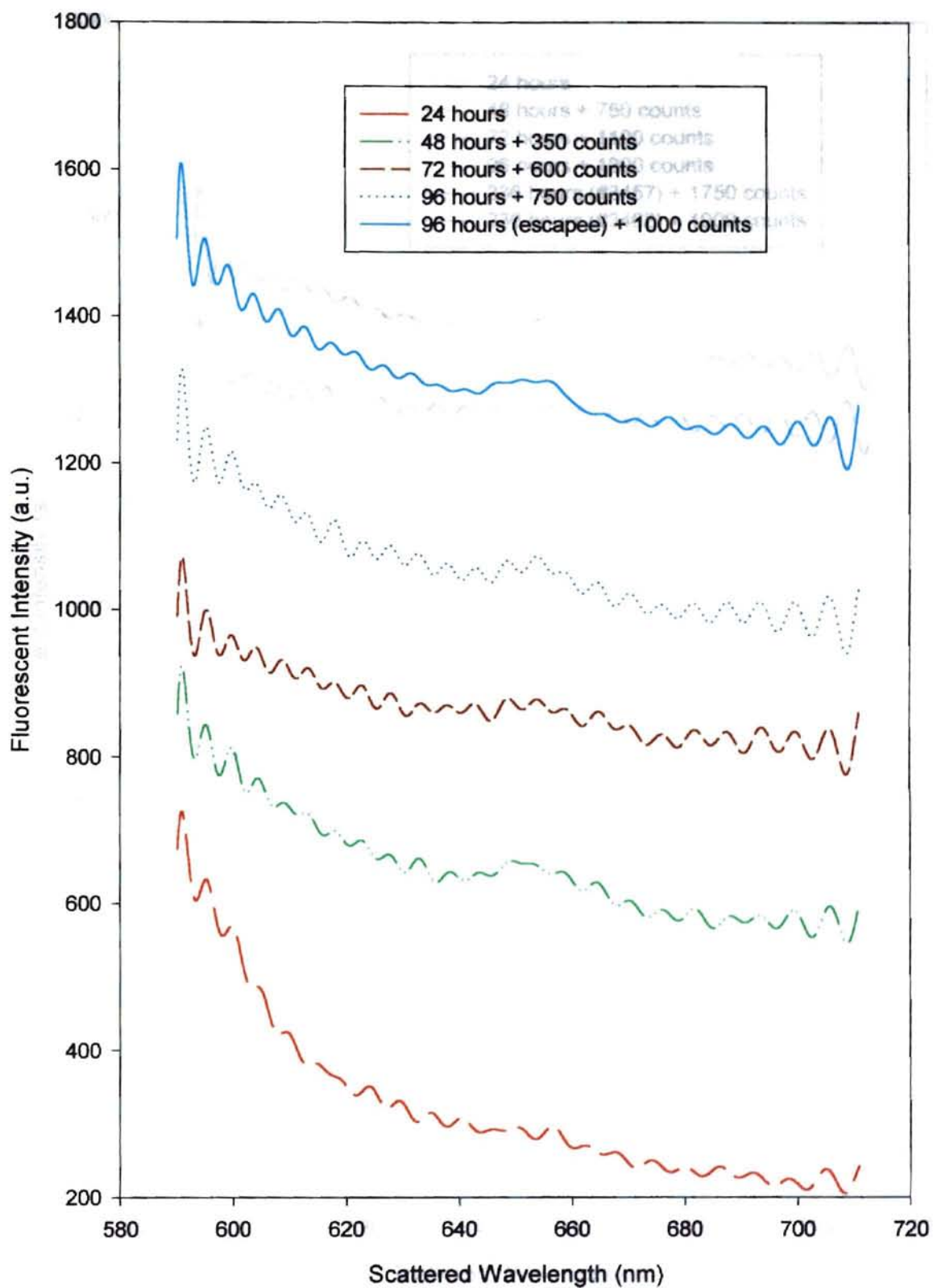


Figure 3.16 Emission spectra of nasal planum injected with 0.15 mg/kg of Foscan®.

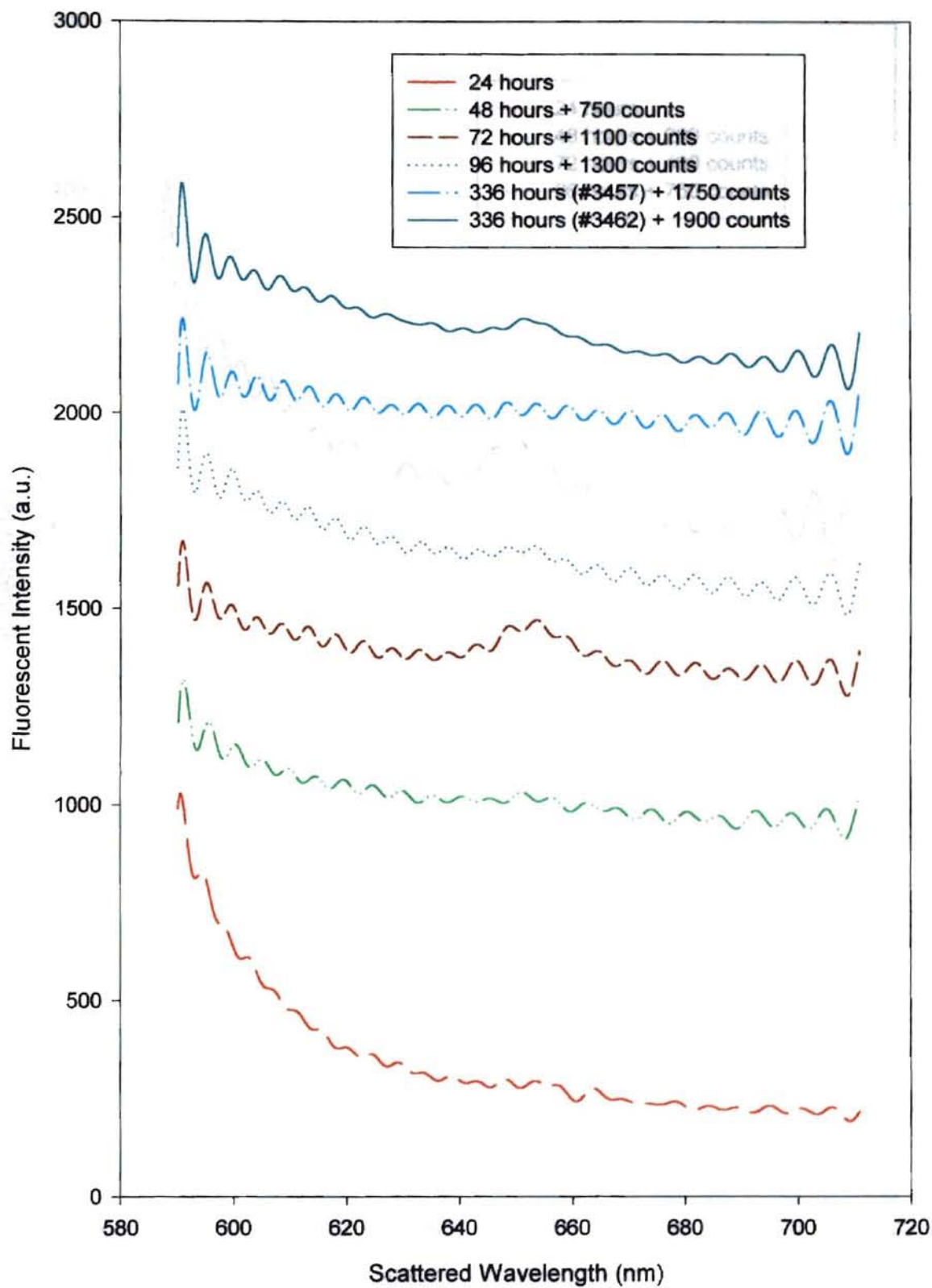


Figure 3.17 Emission spectra of nasal planum injected with 0.30 mg/kg of Foscan®.

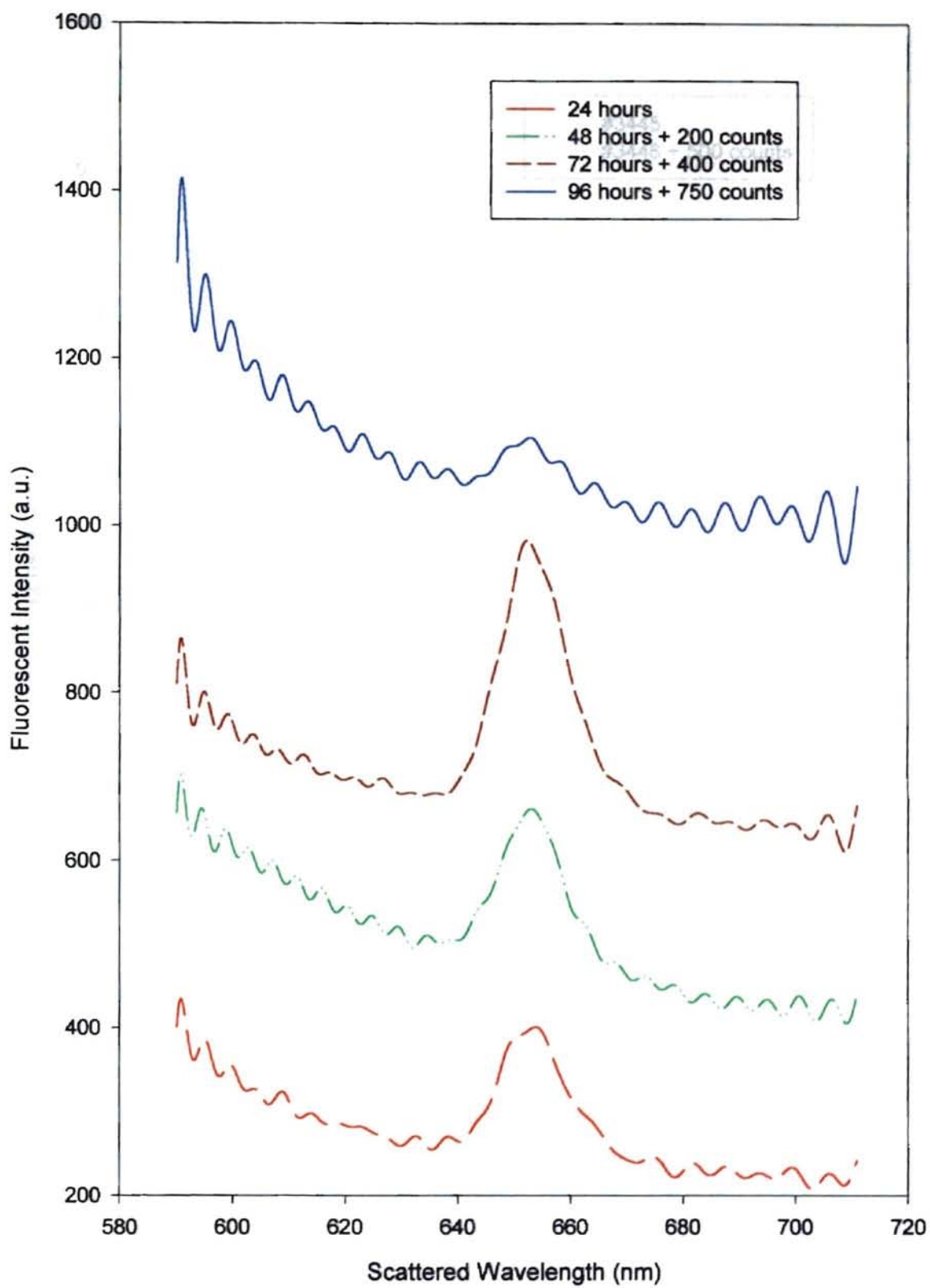


Figure 3.18 Emission spectra of nasal planum injected with 0.60 mg/kg of Foscan®.

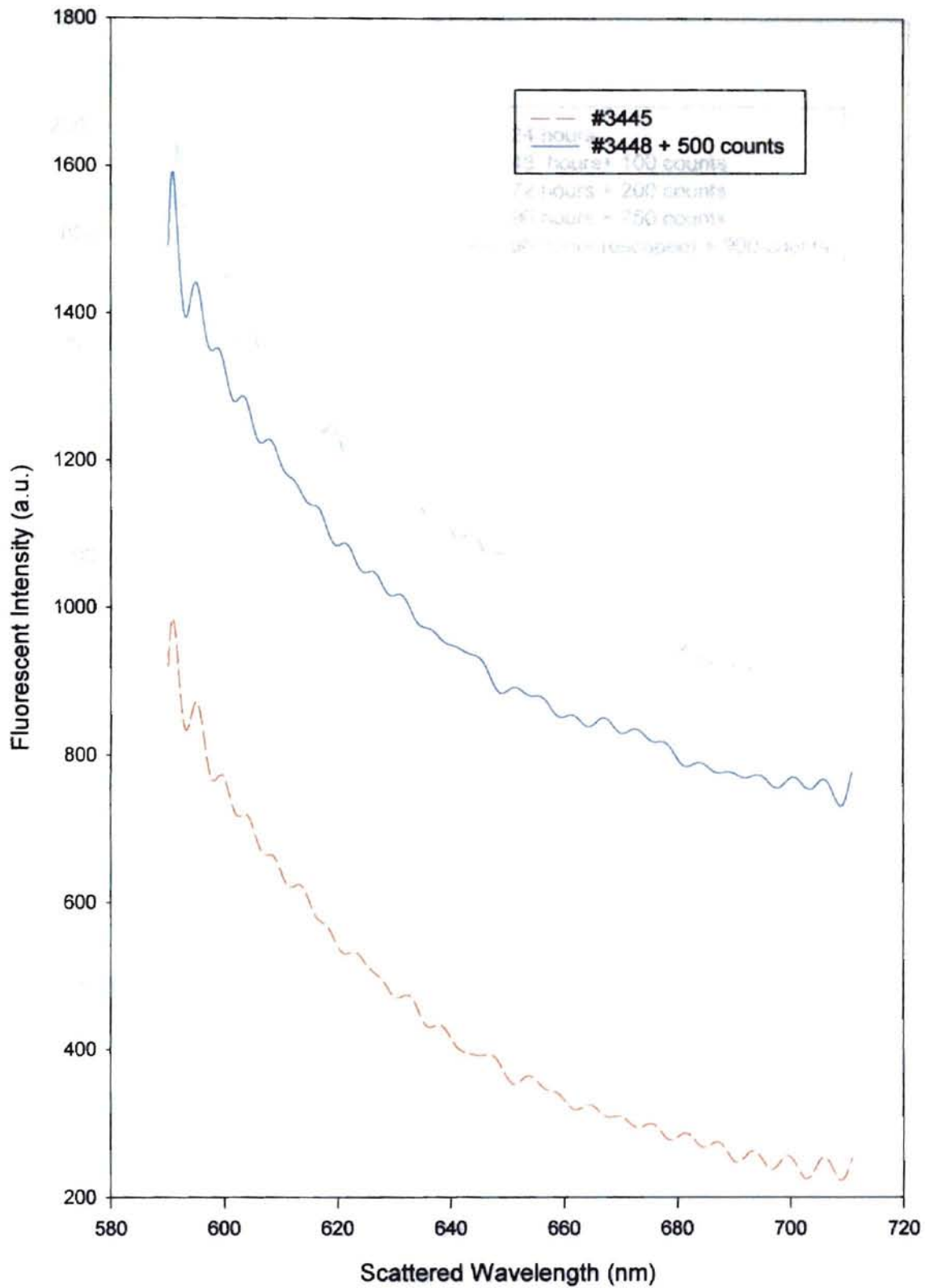


Figure 3.19 Emission spectra of thyroid not injected with Foscan®.

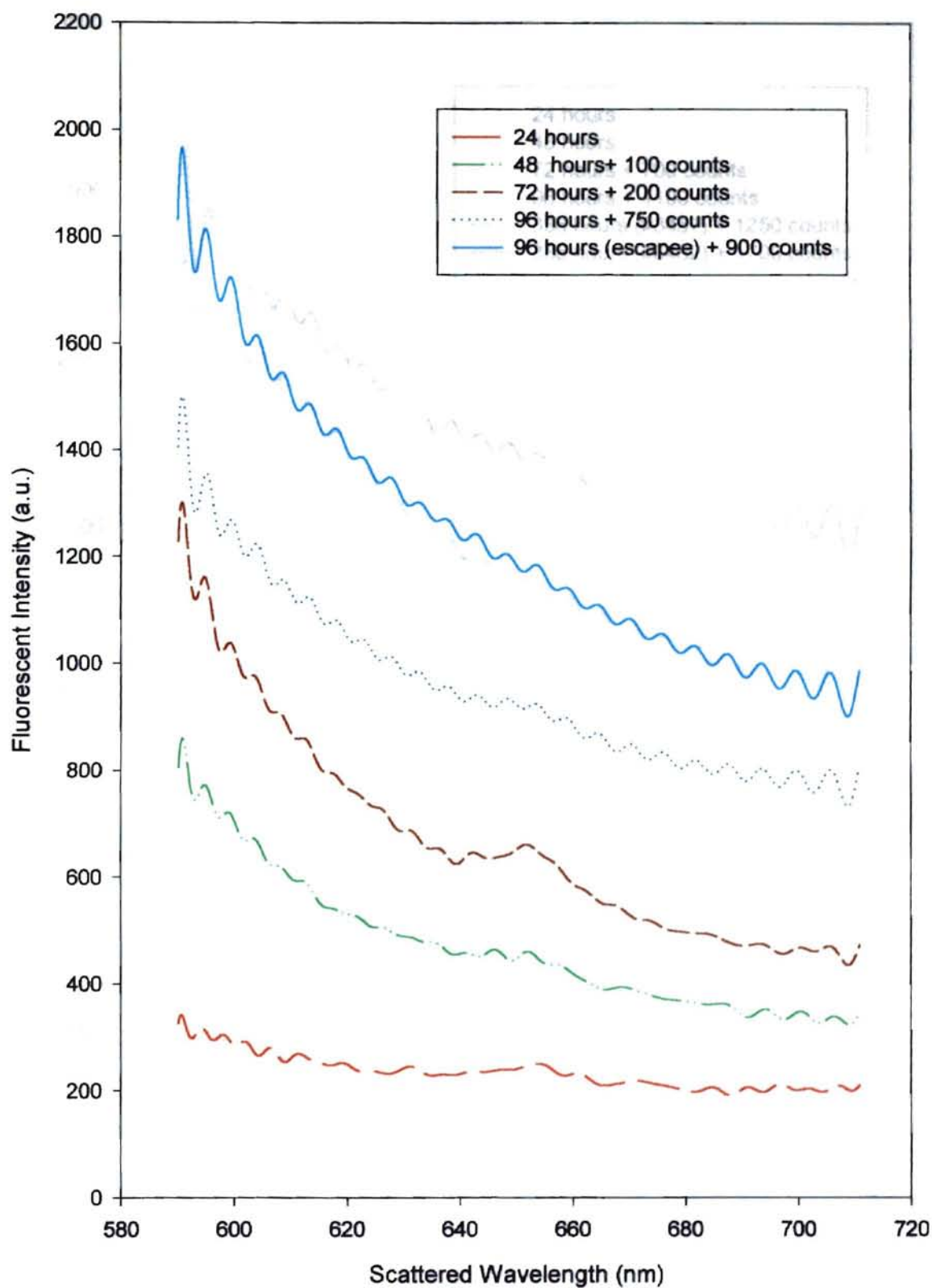


Figure 3.20 Emission spectra of thyroid injected with 0.15 mg/kg of Foscan®.

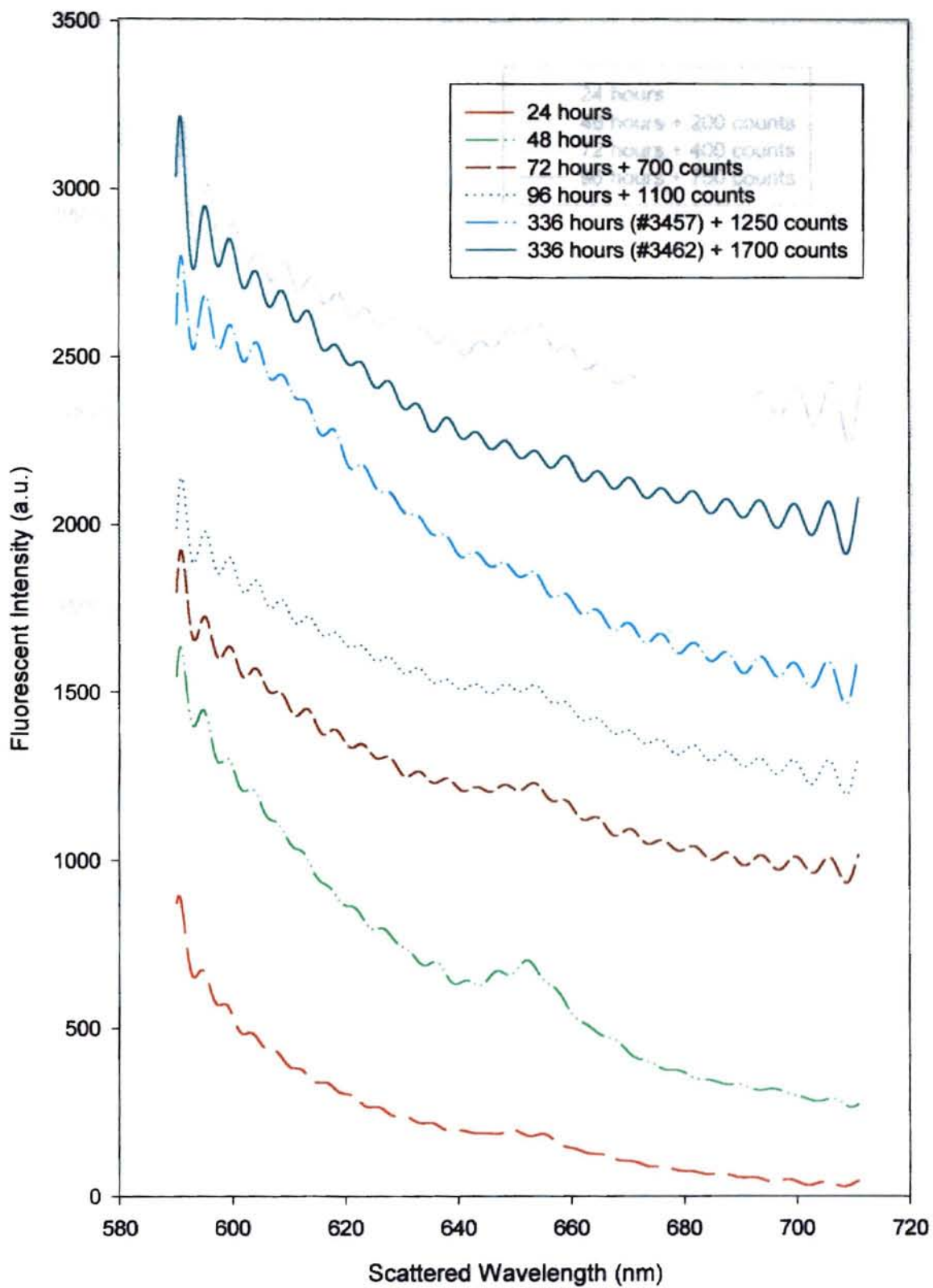


Figure 3.21 Emission spectra of thyroid injected with 0.30 mg/kg of Foscan®.

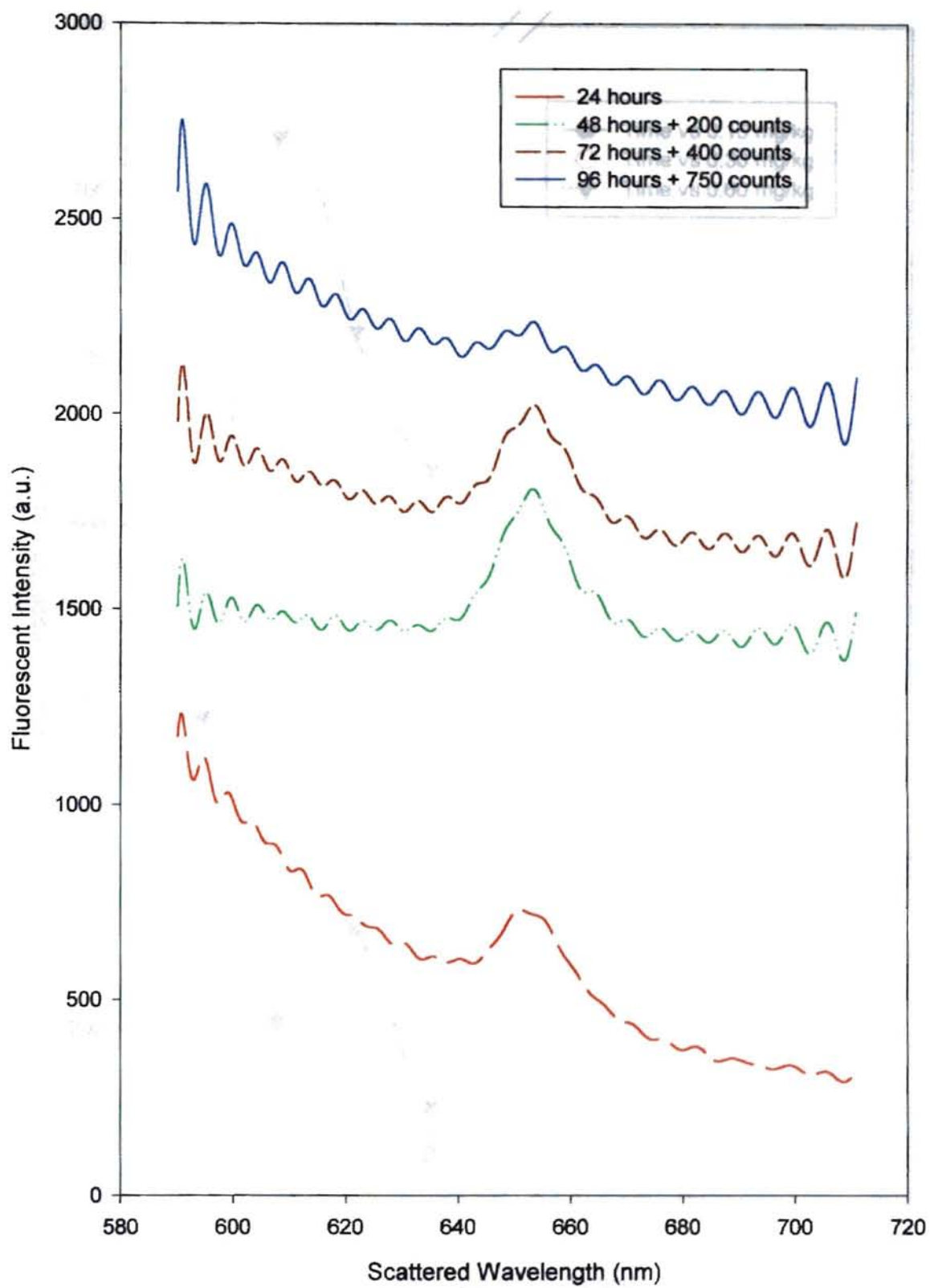


Figure 3.22 Emission spectra of thyroid injected with 0.60 mg/kg of Foscan®.

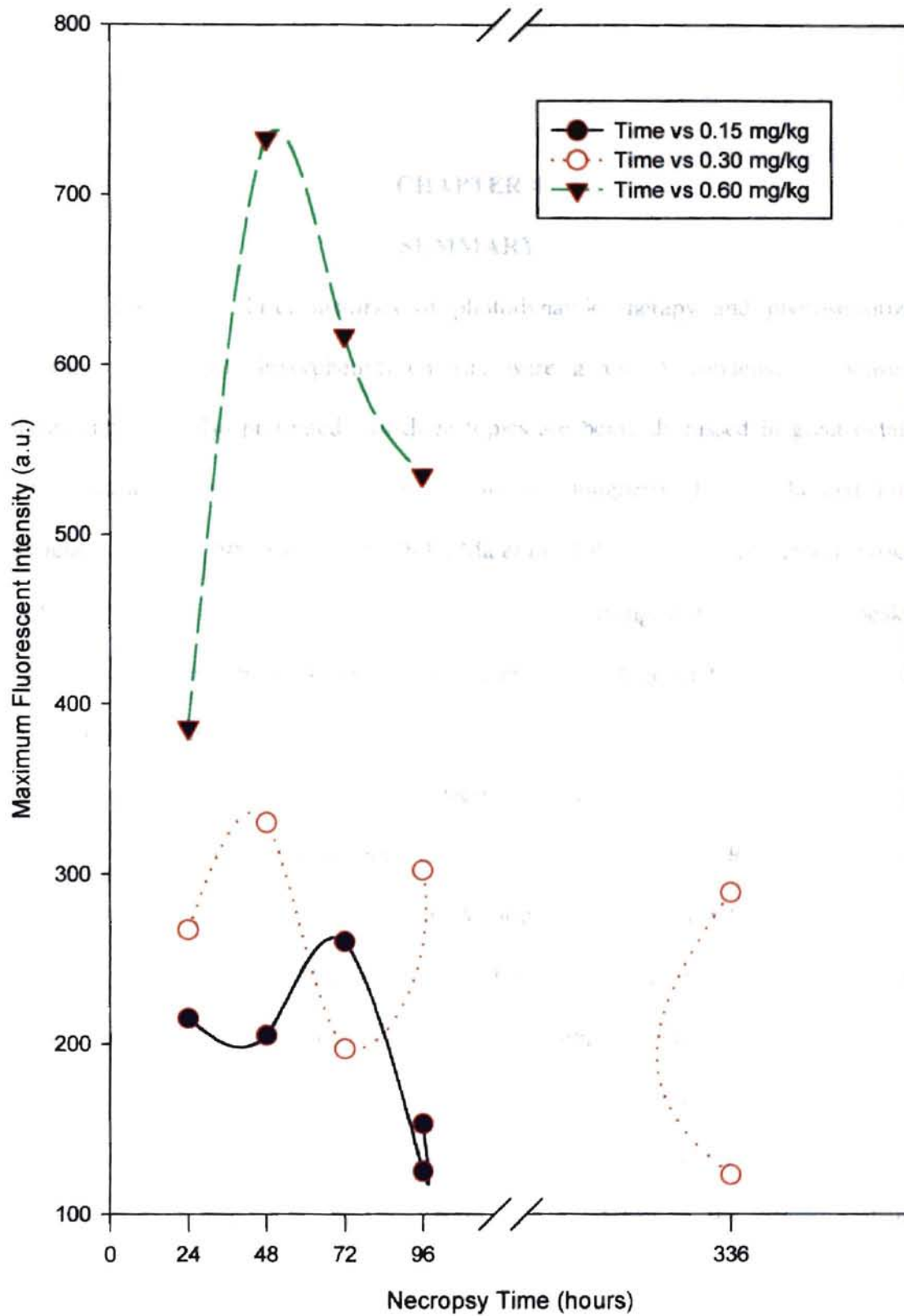


Figure 3.23 Plot of maximum fluorescent intensity versus necropsy time for kidney tissues.

CHAPTER 4

SUMMARY

In Chapter 1, brief histories of photodynamic therapy and photosensitizers, primarily meta-tetra(hydroxyphenyl) chlorin, were given. A condensed synopsis of fluorescence was also presented. All three topics are being discussed in great detail in current literature, especially by such authors as Dougherty, Ronn, Ma and Forrer (Dougherty *et al.*, 1998, Ronn *et al.*, 1997, Ma *et al.*, 1994, Forrer *et al.*, 1991). Foscan[®] has been shown in studies (Alian *et al.*, 1994) to have strong, distinct emission peaks at 652 nm and 718 nm. The peak that is currently most advantageous for PDT with mTHPC is the one at 652 nm.

Using the irradiation and data collection techniques described in Chapter 2, we performed fluorescence experiments on various feline tissues. Results from these experiments were presented in Chapter 3. We found that the larger fluorescent intensity peaks came primarily from the animals injected with the highest dosage of mTHPC (0.60 mg/kg). Animals were sacrificed at various times ranging from 24 to 336 hours. The optimal times to find the largest final concentration were 24 hours for lung and liver, 48 hours for kidney and thyroid and 72 hours for nasal planum. The largest final concentrations of drug, found by Dr. Ronn and displayed in the previous chapter, correspond well with the fluorescent intensity data presented here.

It has been noted in numerous studies (Bonnett *et al.*, 1989, Lofgren *et al.*, 1994, Abramson *et al.*, 1994) that highly vascularized tissues tend to have a higher

concentration of drug, compared to tissues located in regions with weaker capillary arrangements. Of the samples investigated, kidney, liver and lung have a larger blood supply than do the nasal planum and thyroid. Additionally, mTHPC is considered to be a hard drug, in that it is not metabolized but is effectively and nearly completely eliminated via the liver. Thus we expect to see larger intensity peaks in the kidney, liver and lung.

PDT is an ever-evolving treatment strategy. Photosensitizers are being reevaluated every day in hopes that one can be found that will lessen the unintentional damage to surrounding tissues, while still providing maximum therapeutic results to the target tissue. Fluorescence studies play a significant role in this examination. Fluorescence measurements can be taken in vivo, and relatively quickly, allowing on-the-spot diagnosis.

The next step here at Oklahoma State is to construct a calibration curve, using known concentrations of Foscan[®] contained in tissue, so that a measured fluorescent intensity corresponds to a known concentration. This will permit the use of fluorescence intensity measurements for determining the proper time interval to perform PDT in the Boren Veterinary Medical Teaching Hospital.

REFERENCES

1. Abramson, A., Lofgren, L., Ronn, A., Nouri, M., and Steinberg, B., Treatment effects of meta-tetra(hydroxyphenyl)chlorin on the larynx. *New Approaches to Cancer Treatment*, Ed. Horrobin, D., Churchill Communications Europe, London, 142-147, 1994.
2. Alian, W., Andersson-Engels, S., Svanberg, K., and Svanberg, S., Laser-induced fluorescence studies of meso-tetra(hydroxyphenyl)chlorin in malignant and normal tissues in rats. *Br. J. Cancer*, **70**, 880-885, 1994.
3. Andersson, P., Kjellen, E., Montan, S., Svanberg, K., and Svanberg, S., Autofluorescence of various rodent tissues and human skin tumour samples. *Lasers Med Sci*, **2**, 41-49, 1986.
4. Andrejevic-Blant, S., Hadjur, C., Ballini, J., Wagnieres, G., Fontollet, C., van der Bergh, H., and Monnier, P., Photodynamic therapy of early squamous cell carcinoma with tetra(m- hydroxyphenyl)chlorin: optimal drug-light interval. *Br. J. Cancer*, **76**(8), 1021-1028, 1997.
5. Belitchenko, I., Melnikova, V., Bezdetnaya, L., Rezzoug, H., Merlin, J., Potapenko, A., and Guillemin, F., Characterization of photodegradation of meta-tetra(hydroxyphenyl)chlorin (mTHPC) in solution: biological consequences in human tumor cells. *Photochem. Photobiol.*, **67**(5), 584-590, 1998.

6. Benson, R., Meyer, R., Zaruba, M., and McKhann, G., Cellular autofluorescence - is it due to flavins? *J. Histochem. Cytochem.*, **27**(1), 44-48, 1979.
7. Berenbaum, M., Akande, S., Bonnett, R., Kaur, H., Ioannou, S., White, R., and Winfield, U., meso-tetra(hydroxyphenyl)porphyrins, a new class of potent tumour photosensitisers with favourable selectivity. *Br. J. Cancer*, **54**, 717-725, 1986.
8. Berenbaum, M., Comparison of haematoporphyrin derivative and new photosensitizers. In: *Ciba Foundation Symposium 146. Photosensitizing compounds: their chemistry, biology and clinical use*, pp. 33-39, Wiley, Chicester, 1989.
9. Bonnett, R., White, R., Winfield, U., and Berenbaum, M., Hydroporphyrins of the meso-tetra(hydroxyphenyl)porphyrin series as tumor photosensitizers. *Biochem J*, **261**, 277-280, 1989.
10. Braichotte, D., Savary, J., Glanzmann, T., Monnier, P., Wagnieres, G., and van den Bergh, H., Optimizing light dosimetry in photodynamic therapy of the bronchi by fluorescence spectroscopy. *Lasers Med Sci*, **11**, 247-254, 1996a.
11. Braichotte, D., Savary, J., Monnier, P., and van den Bergh, H., Optimizing light dosimetry in photodynamic therapy of early-stage carcinomas of the esophagus using fluorescence spectroscopy. *Lasers Surg Med*, **19**, 340-346, 1996b.
12. Dougherty, T., Cooper, M., and Mang, T., Cutaneous phototoxic occurrences in patients receiving Photofrin®. *Lasers Surg Med*, **10**, 485-488, 1990.
13. Dougherty, T., and Marcus, S., Photodynamic therapy. *Eur. J. Cancer*, **28A**(10), 1734-1742, 1992.
14. Dougherty, T., Review: Photodynamic therapy. *Photochem Photobiol*, **58**(6), 895-900, 1993.

15. Dougherty, T., Gomer, C., Henderson, B., Jori, G., Kessel, D., Korbek, M., Moan, J., and Peng, Q., Photodynamic therapy. *J Natl Cancer Inst*, **90**(12), 889-905, 1998.
16. Forrer, M., Glanzmann, T., Braichotte, D., Wagnieres, G., van den Bergh, H., Savary, J., and Monnier, P., In vivo measurement of fluorescence bleaching of meso-tetrahydroxyphenyl chlorin (mTHPC) in the esophagus and the oral cavity. *SPIE*, **2627**, 33-39, 1991.
17. Glanzmann, T., Hadjur, C., Zellweger, M., Grosjean, P., Forrer, M., Ballini, J., Monnier, P., van den Bergh, H., Lim, C., and Wagnieres, G., Pharmacokinetics of tetra(m-hydroxyphenyl)chlorin in human plasma and individualized light dosimetry in photodynamic therapy. *Photochem. Photobiol.*, **67**(5), 596-602, 1998.
18. Grahn, M., McGuinness, A., Benzie, R., Boyle, R., de Jode, M., Dilkes, M., Abbas, B., and Williams, N., Intracellular uptake, absorption spectrum and stability of the bacteriochlorin photosensitizer 5,10,15,20-tetrakis(m-hydroxyphenyl)bacteriochlorin (mTHPBC). Comparison with 5,10,15,20-tetrakis(m-hydroxyphenyl)chlorin (mTHPC). *J. Photochem. Photobiol. B Biol.*, **37**, 261-266, 1997.
19. Hammer-Wilson, M., Sun, C., Ghahramanlou, M., and Berns, M., In vitro and in vivo comparison of argon-pumped and diode lasers for photodynamic therapy using second-generation photosensitizers. *Lasers Surg Med*, **23**, 274-280, 1998.
20. Hammer-Wilson, M., Ghahramanlou, M., and Berns, M., Photodynamic activity of lutetium-texaphyrin in a mouse tumor system. *Lasers Surg Med*, **24**, 276-284, 1999.
21. Lipson, R., Gray, M., and Baldes, E., Hematoporphyrin derivative for detection and management of cancer. *Ninth Internat. Cancer Congr., Toyko, Japan* p.393. (Abstract), 1966.

22. Lofgren, L., Ronn, A., Abramson, A., Shikowitz, M., Nouri, M., Lee, C., Batti, J., and Steinberg, B., Photodynamic therapy using m-tetra(hydroxyphenyl)chlorin: an animal model. *Arch. Otol. Head & Neck Surg*, **120**(12), 1355-1362, 1994.
23. Ma, L., Moan, J., and Berg, K., Evaluation of a new photosensitizer, meso-tetra-hydroxyphenyl-chlorin, for use in photodynamic therapy: a comparison of its photobiological properties with those of two other photosensitizers. *Int. J. Cancer*, **57**, 883-888, 1994.
24. Mlkvy, P., Hessman, H., MacRobert, A., Pauer, M., Sams, V., Davies, C., Stewart, J., and Bown, S., Photodynamic therapy of a transplanted pancreatic cancer model using meta-tetrahydroxyphenylchlorin (mTHPC). *Br. J. Cancer*, **76**(6), 713-718, 1997.
25. Rezzoug, H., Bezdetnaya, L., A'amar, O., Merlin, J., and Guillemin, F., Parameters affecting photodynamic activity of Foscan® or meta-tetra(hydroxyphenyl)chlorin (mTHPC) in vitro and in vivo. *Lasers Med Sci*, **13**, 119-125, 1998.
26. Ronn, A., Lofgren, L., and Westerborn, A., Interspecies pharmacokinetics as applied to the "hard drug" photosensitizing agent meta(tetrahydroxyphenyl)chlorin. *SPIE Proceedings of Photochemotherapy: Photodynamic Therapy and Other Modalities*, **2625**, 118-123, 1995.
27. Ronn, A., Nouri, M., Lofgren, L., Steinberg, B., Westerborn, A., Windahl, T., Shikowitz, M., and Abramson, A., Human tissue levels and plasma pharmacokinetics of Temoporfin (Foscan®, mTHPC). *Lasers Med Sci*, **11**, 267-272, 1996.

28. Ronn, A., Batti, J., Lee, C., Yoo, D., Siegel, M., Nouri, M., Lofgren, L., and Steinberg, B., Comparative biodistribution of meta-tetra(hydroxyphenyl) chlorin in multiple species: clinical implications for photodynamic therapy. *Laser Surg Med*, **20**, 437-442, 1997.
29. Ronn, A., (unpublished data).
30. Stewart, J., Photosensitizers for photodynamic therapy. *Curr. Opin. Invest. Drugs*, **2**(12), 1279-1289, 1993.
31. Svanberg, S., Medical applications of laser spectroscopy. *Physica Scripta*, **T26**, 90-98, 1989.
32. Weishaupt, K., Gomer, C., and Dougherty, T., Identification of singlet oxygen as the cytotoxic agent in photodestruction of a murine tumor. *Cancer Res*, **36**, 2326-2329, 1976.

VITA

Samuel James Rhoades IV

Candidate for the Degree of

Master of Science

Thesis: FLUORESCENCE SPECTROSCOPY OF FOSCAN[®] INDUCED FELINE TISSUES.

Major Field: Natural and Applied Sciences

Specialization: Biophotonics

Biographical:

Personal Data: Born in Oklahoma City, Oklahoma on April 12, 1975, the son of Sam and Becky Rhoades.

Education: Graduated from Bishop Kelley High School, Tulsa, Oklahoma in May, 1993; received Bachelor of Science degree in Physics from Loyola University, New Orleans, Louisiana in May, 1997. Completed the requirements for the Master of Science degree with a major in Physics at Oklahoma State University in December, 1999.

Professional Experience: Employed as an undergraduate research assistant; Oklahoma State University, summer 1996. Employed as a graduate teaching assistant; Oklahoma State University, 1997-1998. Employed as a graduate research assistant; Oklahoma State University, 1998-present.

Professional Memberships: Sigma Xi Research Society, the American Physical Society and the American Association for the Advancement of Science.